Manganese scavenging and oxidative stress response mediated by type VI secretion system in *Burkholderia thailandensis*

Meiru Si[a,b], Chao Zhao[a], Brianne Burkinshaw[c], Bing Zhang[a], Dawei Wei[a], Yao Wang[a], Tao G. Dong[c,1], and Xihui Shen[a,1]

[a]State Key Laboratory of Crop Stress Biology for Arid Areas and College of Life Sciences, Northwest A&F University, Yangling, Shaanxi 712100, China; [b]College of Life Sciences, Qufu Normal University, Qufu, Shandong 273165, China; and [c]Ecosystem and Public Health, Faculty of Veterinary Medicine, University of Calgary, Calgary, AB, Canada T2N 4Z6

Edited by Thomas J. Silhavy, Princeton University, Princeton, NJ, and approved February 6, 2017 (received for review September 8, 2016)

Type VI secretion system (T6SS) is a versatile protein export machinery widely distributed in Gram-negative bacteria. Known to translocate protein substrates to eukaryotic and prokaryotic target cells to cause cellular damage, the T6SS has been primarily recognized as a contact-dependent bacterial weapon for microbe–host and microbial interspecies competition. Here we report contact-independent functions of the T6SS for metal acquisition, bacteria competition, and resistance to oxidative stress. We demonstrate that the T6SS-4 in *Burkholderia thailandensis* is critical for survival under oxidative stress and is regulated by OxyR, a conserved oxidative stress regulator. The T6SS-4 is important for intracellular accumulation of manganese (Mn^{2+}) under oxidative stress. Next, we identified a T6SS-4–dependent Mn^{2+}-binding effector TseM, and its interacting partner MnoT, a Mn^{2+}-specific TonB-dependent outer membrane transporter. Similar to the T6SS-4 genes, expression of *mnoT* is regulated by OxyR and is induced under oxidative stress and low Mn^{2+} conditions. Both TseM and MnoT are required for efficient uptake of Mn^{2+} across the outer membrane under Mn^{2+}-limited and -oxidative stress conditions. The TseM–MnoT-mediated active Mn^{2+} transport system is also involved in contact-independent bacteria–bacteria competition and bacterial virulence. This finding provides a perspective for understanding the mechanisms of metal ion uptake and the roles of T6SS in bacteria–bacteria competition.

type VI secretion | outer membrane transporter | ion uptake | oxidative stress | *Burkholderia*

Manganese (Mn^{2+}) is an essential micronutrient transition metal required for many cellular processes, including intermediary metabolism, transcriptional regulation, and particularly resistance to oxidative stress (1, 2). Manganese mitigates oxidative stress by serving as a cofactor for reactive oxygen species (ROS)-detoxifying enzymes (i.e., the superoxide dismutase SodA and the catalase KatN) and through the formation of nonproteinaceous manganese antioxidants in a large variety of organisms (1–4). Manganese can also enhance oxidative stress resistance by replacing the more reactive iron cofactor in certain iron-containing enzymes susceptible to oxidative attack (5). Given the essential role of Mn^{2+} in bacterial physiology, it is not surprising that restriction of this micronutrient is an important innate defense strategy. Indeed, Mn^{2+} is strictly sequestered by a defense mechanism termed nutritional immunity in mammalian hosts (6–8). To acquire sufficient Mn^{2+} concentrations for adaptation to environmental stress and pathogenesis within the host niche, bacteria have developed a number of Mn^{2+} transporters. The import of Mn^{2+} across the inner membrane is primarily mediated by either the ATP-binding cassette (ABC) family transporter exemplified by SitABCD (9, 10), or the natural resistance-associated macrophage protein (NRAMP) family transporter exemplified by MntH (11–13). Recently, Hohle et al. (14) described a Mn^{2+}-selective channel protein, MnoP, which facilitates passive transport of free Mn^{2+} across the outer membrane of *Bradyrhizobium japonicum*. However, to date, an active transporter for translocation of Mn^{2+} across the outer membrane has not been described.

The type VI secretion system (T6SS) is a widespread protein export apparatus used by many Gram-negative bacteria to translocate effector proteins into eukaryotic or prokaryotic cells in a contact-dependent manner (15–18). Many species possess multiple evolutionarily distinct T6SSs, which are found to play versatile physiological roles in areas such as acute and chronic infections, interbacterial interactions, biofilm formation, and stress response (15, 19–23). A well-established function of the T6SSs is to compete against rival bacteria in polymicrobial environments by delivering "antibacterial" toxins such as cell-wall–degrading enzymes, nucleases, and membrane-targeting enzymes, into target competitor bacterial cells (24–27). Moreover, some T6SSs associated with pathogens have been reported to be involved in bacterial pathogenesis by translocating "antieukaryotic" effectors into eukaryotic cells to modulate host immunity and inflammation (28–31). The well-characterized antieukaryotic effectors are several "evolved" VgrG proteins and non-VgrG phospholipases and deamidases (28–31). Recently, we reported that the T6SS-4 from *Yersinia pseudotuberculosis* was involved in zinc transport via secretion of the zinc-chelating effector YezP into medium (32). Although the underlying mechanisms remain unknown, this finding uncovers a function of T6SS in increasing bacterial fitness by competition for essential nutrients and reducing ROS. This finding also raises the question of whether T6SS can transport other metal ions such as

Significance

As an essential micronutrient, Gram-negative bacteria must concentrate Mn^{2+} into the cytosol via active transport systems to meet cellular demands. Whereas inner membrane Mn^{2+} transporters have been characterized, an active transporter for translocation of Mn^{2+} across the outer membrane has not been described. Here we report a Mn^{2+}-scavenging pathway consisting of a newly identified TonB-dependent outer membrane manganese transporter, MnoT, and a type VI secretion system (T6SS)-secreted Mn^{2+}-binding protein, TseM. Traditionally, T6SS is recognized as a contact-dependent nanomachine to inject effectors into eukaryotic or prokaryotic cells for virulence or for interbacterial competition. The contact-independent functions of T6SS for metal acquisition and bacteria–bacteria competition, reported here, suggest that T6SS may have been retrofitted by some bacteria to gain additional adaptive functions during evolution.

Author contributions: Y.W., T.G.D., and X.S. designed research; M.S., C.Z., B.Z., and D.W. performed research; Y.W. and X.S. contributed new reagents/analytic tools; M.S., B.B., Y.W., T.G.D., and X.S. analyzed data; and M.S., T.G.D., and X.S. wrote the paper.

The authors declare no conflict of interest.

This article is a PNAS Direct Submission.

[1]To whom correspondence may be addressed. Email: xihuishen@nwsuaf.edu.cn or tdong@ucalgary.ca.

This article contains supporting information online at www.pnas.org/lookup/suppl/doi:10.1073/pnas.1614902114/-/DCSupplemental.

Mn^{2+}, which plays crucial roles in detoxification of ROS in microorganisms.

Burkholderia thailandensis, a soil bacterium nonpathogenic to humans, is often used as a model organism for *Burkholderia pseudomallei*, the causative agent of the severe disease melioidosis (33, 34). *B. pseudomallei* is highly resistant to numerous antibiotics and is listed as a category B priority pathogen and a tier 1 select agent for its potential use as a biological weapon. Whereas the genomes of many bacteria harbor one to two T6SS gene clusters (22, 35), the closely related *B. thailandensis* and *B. pseudomallei* contain five and six such clusters, respectively, suggesting multiple functions or specificities for particular niches or hosts. In *Burkholderia thailandensis*, T6SS-5 was found to play a critical role in the virulence of the organism in a murine melioidosis model, and T6SS-1 was found to be required for contact-dependent interbacterial competition (22). However, the function of other such transporters remains enigmatic.

We here demonstrate that OxyR, a conserved oxidative stress regulator, regulates the T6SS-4 in *B. thailandensis*, which in turn facilitates the uptake of Mn^{2+} to mitigate oxidative stress through secreting a Mn^{2+}-binding effector TseM. Uptake of TseM-bound Mn^{2+} requires a TonB-dependent outer membrane transporter (TBDT), MnoT, for active transport across the outer membrane under Mn^{2+}-limited and oxidative stress conditions. Because TseM is the first reported proteinaceous nonhemopore metallophore recognized by TBDT, this finding greatly expands our understanding of active metal ion transport in bacteria. Metal assimilation and oxidative stress resistance mediated by the T6SS confers a contact-independent competitive advantage distinct from those well-studied T6SS-mediated contact-dependent functions, suggesting its diverse physiological functions have yet to be fully appreciated in Gram-negative bacteria.

Results

OxyR Negatively Regulates T6SS-4 Expression in *B. thailandensis*. OxyR is a known regulator for oxidative stress in many bacterial species but its role in *B. thailandensis* has not been characterized. Here we found that the *B. thailandensis* Δ*oxyR* mutant showed increased resistance compared with the wild-type and the complement strain upon cumene hydroperoxide (CHP), H_2O_2, $CdCl_2$, and diamide challenge (Fig. S1*A*). However, deletion of *oxyR* did not affect bacterial growth under normal condition (Fig. S1*B*). This finding indicates that *B. thailandensis* OxyR negatively regulates cellular defense genes against oxidative stress. To systematically identify OxyR-controlled genes, we performed RNA sequencing (RNA-seq)-based transcriptomic analysis and identified 673 differentially expressed genes either induced or repressed at least 1.6-fold (Dataset S1). We then validated the transcriptomic data using quantitative reverse transcriptase PCR (qRT-PCR) analysis on 14 representative genes (Fig. 1*A*). Interestingly, similar to the known target genes

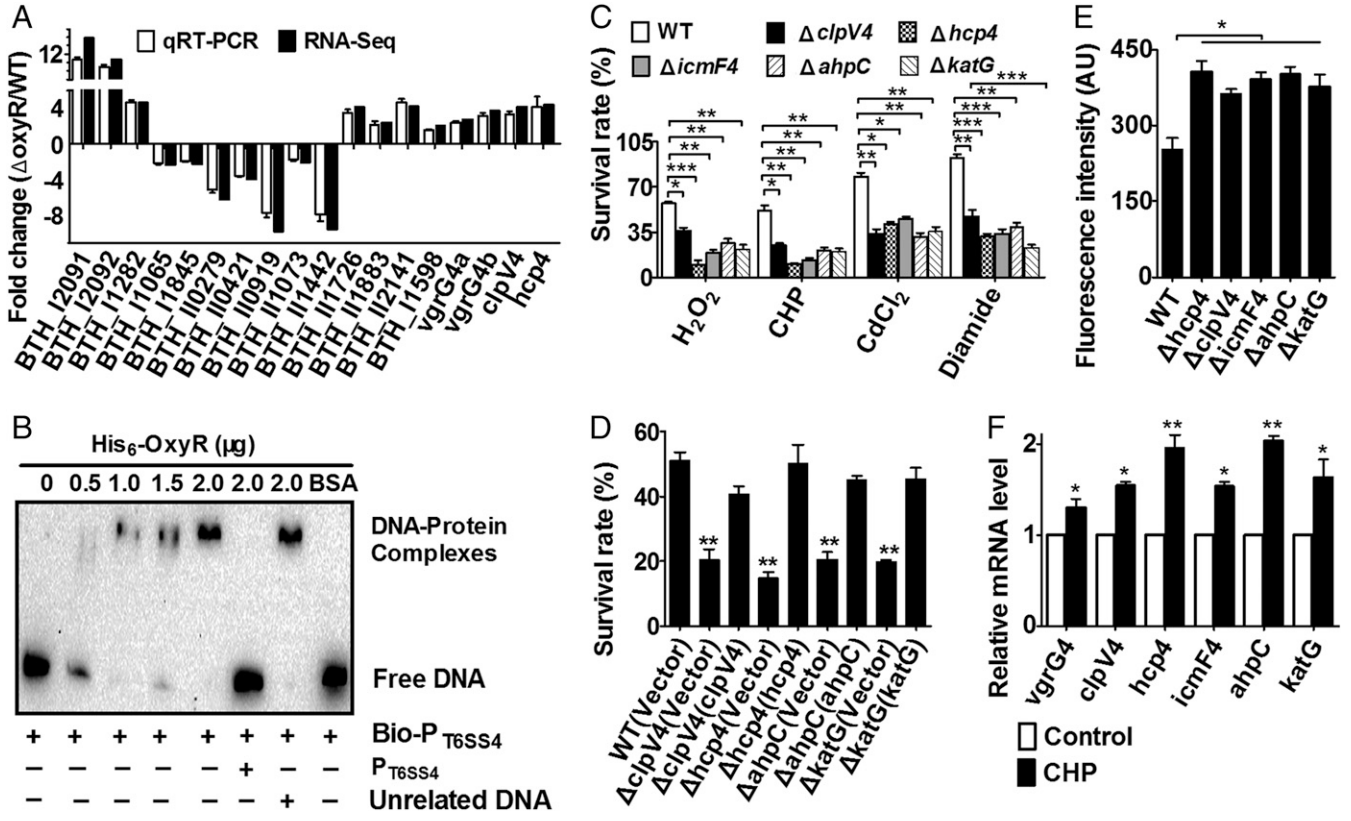

Fig. 1. OxyR-regulated T6SS-4 is involved in oxidative stress resistance. (*A*) Genes differentially transcribed in the *B. thailandensis oxyR* mutant compared with those in the wild type were detected by transcriptomic and qRT-PCR analyses. Fourteen representative genes were chosen to validate the RNA-seq data by qRT-PCR. The white bars represent the mean values obtained for the reference wild type and three biological replicates. Error bars indicate the SD. Black bars represent RNA-seq data. (*B*) Binding of OxyR to the T6SS-4 promoter. Interaction of OxyR with a biotin-labeled probe was detected using streptavidin-conjugated HRP and a chemiluminescent substrate. An unlabeled promoter was added to determine the binding specificity of OxyR. Bio-P_{T6SS-4}, biotin-labeled T6SS-4 promoter. (*C* and *D*) The indicated strains grown to the stationary phase were exposed to diverse stress for 40 min and the viability of the cells was determined. Data shown are the average and SD from three independent experiments. (*E*) Deletion of T6SS-4 led to accumulation of intracellular ROS under oxidative conditions. Intracellular ROS in stationary phase bacterial strains exposed to CHP was determined with the H_2DCFDA probe. Data shown are the average and SD from three independent experiments. (*F*) Oxidative stress induced the expression of T6SS-4. *B. thailandensis* strains were treated with the indicated amounts of CHP and the expressions of the major components of T6SS-4 were measured by qRT-PCR. Data shown are the average and SD from three independent experiments. ***$P \leq 0.001$; **$P \leq 0.01$; *$P \leq 0.05$.

of OxyR, including *ahp*C (*bth_I2092*) and *katG* (*bth_I1282*), most genes encoding the major components of T6SS-4 showed significantly enhanced transcription in the Δ*oxyR* mutant compared with that in the wild type (Dataset S1). Negative regulation of T6SS-4 component genes (*vgrG4a*, *vgrG4b*, *clpV4*, and *hcp4*) by OxyR was also confirmed by qRT-PCR analysis (Fig. 1*A*). The negative regulation of T6SS-4 by OxyR was derepressed upon CHP challenge (Fig. S1 *C* and *D*). The results indicate that OxyR functions as a general transcriptional repressor similar to the OxyR homologs in *B. pseudomallei* (36), *Neisseria gonorrheae* (37), and *Corynebacterium glutamicum* (38).

To determine whether OxyR regulates T6SS-4 expression directly, we examined the interaction between OxyR and the T6SS-4 promoter using an electrophoretic mobility shift assay (EMSA). Incubation of a probe containing the T6SS-4 promoter (P_{T6SS-4}) sequence (−536 to −186 relative to the ATG start codon of the first ORF of the T6SS-4 operon) with His_6-OxyR led to the formation of DNA–protein complexes, and addition of excessive unlabeled probe abolished the formation of the protein–DNA complex (Fig. 1*B*). Consistently, a DNA element highly similar to the known recognition site for OxyR was identified in the T6SS-4 promoter region (Fig. S1*E*). Thus, OxyR negatively regulates T6SS-4 expression by specifically recognizing an operator within the T6SS-4 promoter.

The direct regulation of T6SS-4 by OxyR prompted us to examine whether the T6SS-4 plays a role in protection against oxidative stress. Thus, we determined the viability of *B. thailandensis* T6SS-4 mutants challenged with diverse oxidative stressors such as CHP, H_2O_2, $CdCl_2$, and diamide. Similar to the Δ*katG* and Δ*ahpC* mutants, all mutants lacking conserved T6SS-4 structural genes were significantly more sensitive to these stressors than wild-type bacteria (Fig. 1*C*). Moreover, the sensitivity of the Δ*clpV4* and Δ*hcp4* mutants to CHP was almost completely alleviated by complementation of the *clpV4* and *hcp4* genes, respectively (Fig. 1*D*), further supporting the role of T6SS-4 in combating oxidative stresses. For simplicity, we used CHP only as the oxidative stressor in the following experiments.

Oxidative stress induces the production of harmful ROS. To examine the effect of T6SS-4 on ROS reduction upon oxidative stress, we assessed the intracellular ROS levels in *B. thailandensis* wild-type and mutant strains challenged with CHP by using the fluorogenic probe 2′,7′-dichlorodihydrofluorescein diacetate (H_2DCFDA). As shown in Fig. 1*E*, mutants lacking essential components of T6SS-4 had significantly higher ROS levels than the wild type after exposure to CHP, indicating that T6SS-4 is critical in reducing ROS accumulated in *B. thailandensis* under stress conditions (Fig. 1*E*). In agreement with these observations, the expression of T6SS-4 component genes was also induced by CHP along with *katG* and *ahpC* (Fig. 1*F*). Altogether, these data indicate that the T6SS-4 is induced and important for survival under oxidative stress.

T6SS-4 Combats Oxidative Stress by Importing Mn^{2+}. Manganese is known to play crucial roles in protection against oxidative damage (1–5). Our observation that *B. thailandensis* T6SS-4 has antioxidant function prompted us to examine whether it is involved in Mn^{2+} acquisition for oxidative stress survival. As shown in Fig. 2*A*, whereas exogenous Mn^{2+} (0.25 μM) markedly increased the survival rate of the wild-type and the complemented strain Δ*clpV4*(*clpV4*) under CHP challenge, the protective effect of exogenous Mn^{2+} was largely abolished in the Δ*clpV4* mutant. In addition, exogenous Mn^{2+} significantly reduced intracellular ROS levels in the wild-type and the complemented strain, whereas a lesser effect was observed in the Δ*clpV4* mutant (Fig. 2*B*). These results suggest that T6SS-4 plays a role in the transport of Mn^{2+} for survival under oxidative stress.

We then postulated that the growth of the Δ*clpV4* mutant might be affected by Mn^{2+} starvation under oxidative conditions. This prediction was confirmed by comparing the growth of the

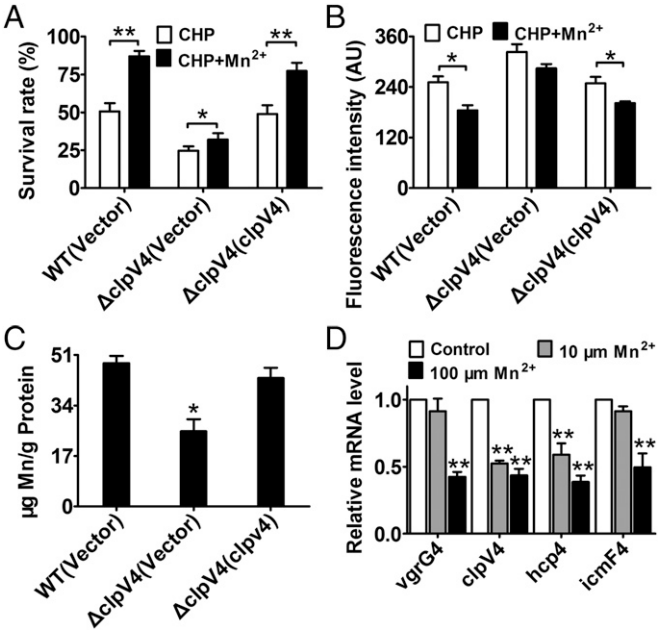

Fig. 2. T6SS-4 is important for the accumulation of intracellular Mn^{2+} under oxidative stress conditions. (*A*) The alleviation of the sensitivity of *B. thailandensis* strains to CHP by exogenous Mn^{2+} (0.25 μM) required T6SS-4. Relevant stationary phase bacterial strains were exposed to 0.25 mM CHP in M9 medium with or without exogenously provided Mn^{2+} (0.25 μM) for 40 min and the viability of the cells was determined. The mean values and SDs from at least three repeats are shown. (*B*) Reduction of intracellular ROS in CHP-treated *B. thailandensis* strains by exogenous Mn^{2+} (0.25 μM) required T6SS-4. The mean values and SD from at least three repeats are shown. (*C*) Mn^{2+} uptake required T6SS-4 under oxidative stress conditions. Stationary phase *B. thailandensis* strains were exposed to 0.25 mM CHP for 20 min in PBS containing 0.25 μM $MnSO_4$. Mn^{2+} associated with bacterial cells was measured by inductively coupled plasmon resonance atomic absorption spectrometry (ICP-MS). (*D*) T6SS-4 expression is inhibited under high Mn^{2+} conditions. *B. thailandensis* wild type was grown in LB containing 10 or 100 μM Mn^{2+}, and the expression of the major T6SS-4 genes was measured by qRT-PCR. Data shown are the average of three independent experiments and error bars indicate the SD from three independent experiments. $^{**}P \leq 0.01$; $^{*}P \leq 0.05$.

B. thailandensis wild type, the Δ*clpV4* mutant, and the complemented strain Δ*clpV4*(*clpV4*) in the presence of ethylene diamine tetraacetic acid (EDTA) under CHP stress (Fig. S2 *A* and *B*). Whereas the levels of growth of all tested strains were nearly identical in lysogeny broth (LB) medium and LB containing EDTA (Fig. S2*A*), the growth of the Δ*clpV4* mutant was severely impaired in comparison with that of the wild-type in LB medium containing EDTA under CHP treatment (Fig. S2*B*). The plasmid-borne expression of *clpV4* completely rescued the sensitivity of the Δ*clpV4* mutant to CHP (Fig. S2*B*). Moreover, although the growth of all strains was improved by the addition of excessive Mn^{2+} (250 μM) under CHP treatment, the level of increase was less in the Δ*clpV4* mutant than in the wild-type and the complemented strain Δ*clpV4*(*clpV4*) (Fig. S2*B*).

To test whether the increased T6SS-4–dependent survival is due to Mn^{2+} acquisition, we measured the total metal content in bacterial cells treated with CHP using inductively coupled plasmon resonance atomic absorption spectrometry (ICP-MS). Our results revealed that deletion of the *clpV4* significantly lowered intracellular Mn^{2+} levels and that the complementation of *clpV4* restored such defects (Fig. 2*C*). Consistent with its role in Mn^{2+} acquisition, the expression of T6SS-4 genes was repressed by exogenous Mn^{2+} in a dose-dependent manner (Fig. 2*D*). Altogether, these data demonstrate that the T6SS-4 mitigates oxidative stress through the uptake of antioxidant manganese.

T6SS-4 Secretes a Mn^{2+}-Binding Protein Substrate. Previously, we showed that zinc transport by *Y. pseudotuberculosis* T6SS-4 can be achieved by secreting a zinc scavenger YezP located at the end of the T6SS-4 gene cluster (32). Here we identified a 154-residue protein (BTH_II1883) encoded by a gene also located at the end of the *B. thailandensis* T6SS-4 gene cluster (Fig. S3*A*). Moreover, no putative promoter was identified upstream of the BTH_II1883 ORF, suggesting that this gene is part of the T6SS-4 operon. This finding prompted us to examine whether BTH_II1883 is a secreted substrate of T6SS-4. As shown in Fig. 3*A*, significant amounts of BTH_II1883 were readily detected in the culture supernatant of wild-type bacteria recognized by a specific anti-BTH_II1883 rabbit polyclonal antibody (Fig. 3*A*). Deletion of *clpV4* abrogated the secretion

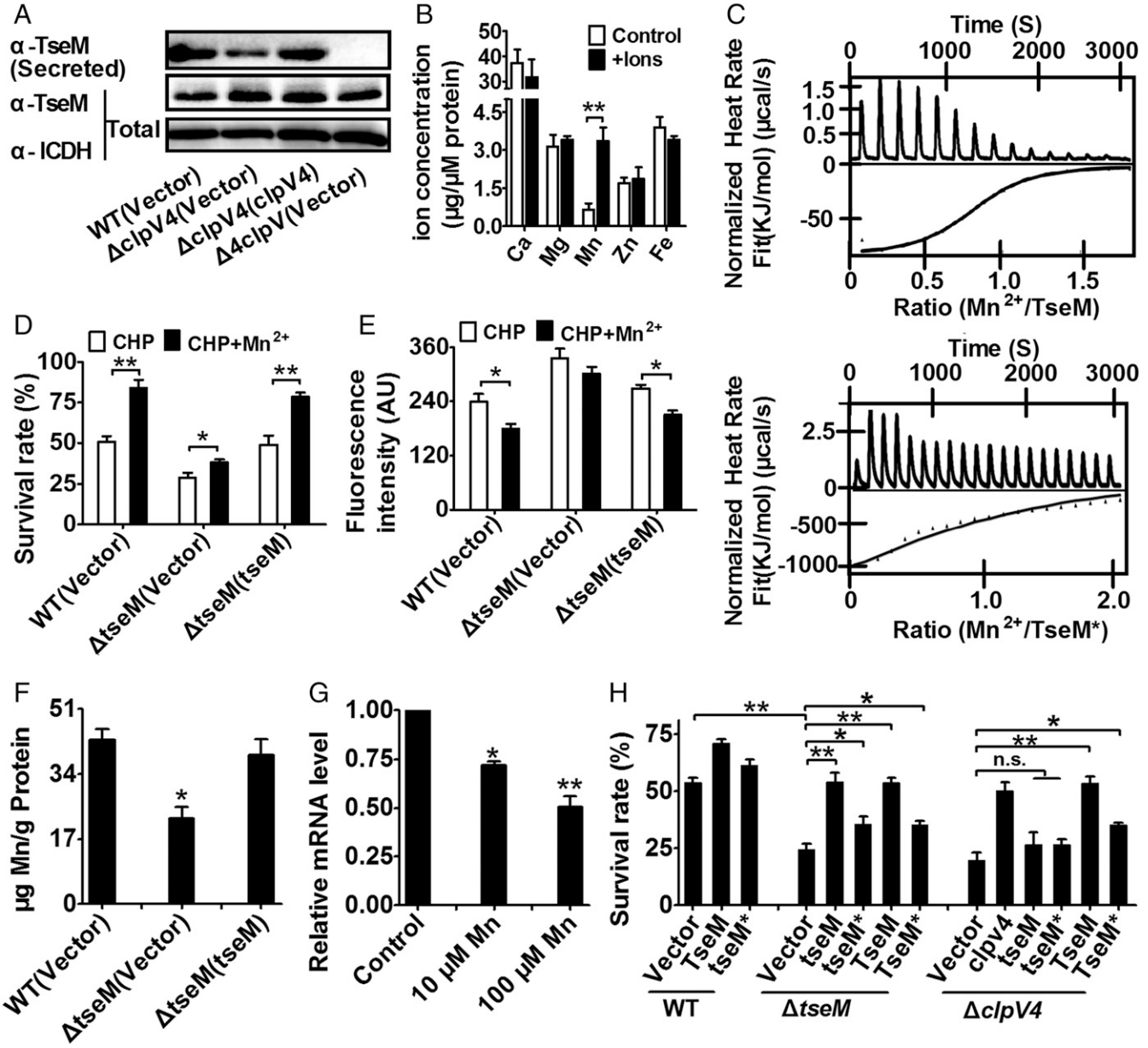

Fig. 3. A Mn^{2+}-binding protein translocated by T6SS-4 resisted oxidative stress. (*A*) TseM is a secreted substrate of T6SS-4. Proteins in culture supernatant of the relevant *B. thailandensis* strains were probed using specific anti-TseM antibody. For the pellet fraction, isocitrate dehydrogenase (ICDH) was used as a loading control. (*B*) The binding of divalent ions by TseM was detected by atomic absorption spectrometry. (*C*) The binding of Mn^{2+} by TseM. Mn^{2+}-free TseM (*Upper*) or TseM* ($TseM^{Q35R/H63A/N132R}$) (*Lower*) was used to evaluate Mn^{2+}-binding activity by isothermal titration calorimetry (ITC). Data were analyzed using the NanoAnalyze software (TA Instruments). (*D*) The alleviation of the sensitivity of *B. thailandensis* strains to CHP by exogenous Mn^{2+} (0.25 μM) required the TseM protein. The viability of stationary phase *B. thailandensis* strains was determined after exposure to CHP, or CHP and 0.25 μM Mn^{2+} for 40 min. (*E*) Deletion of the *tseM* gene led to an accumulation of intracellular ROS. The intracellular levels of ROS were determined with the H_2DCFDA probe after stationary phase *B. thailandensis* strains were exposed to CHP, or CHP with 0.25 μM Mn^{2+} for 40 min. (*F*) TseM is involved in Mn^{2+} acquisition. Stationary phase *B. thailandensis* strains were exposed to 0.25 mM CHP for 20 min in PBS containing 0.25 μM $MnSO_4$. Mn^{2+} associated with bacterial cells was determined by ICP-MS. (*G*) TseM expression is inhibited by high Mn^{2+} conditions. *B. thailandensis* wild-type cells were grown in LB medium with 10 and 100 μM Mn^{2+}, and the expression of *tseM* was measured using qRT-PCR. (*H*) The rescue of the *tseM* or *clpV4* mutant using recombinant TseM protein. Recombinant TseM or TseM* ($TseM^{Q35R/H63A/N132R}$) protein at 1 μM was added to bacterial survival experiments in M9 medium before viability assessment. Mutants complemented with the corresponding gene were used as controls. The mean values and SDs from at least three repeats are shown. $^{**}P \leq 0.01$; $^{*}P \leq 0.05$; n.s., not significant.

of BTH_II1883 to a large extent. The secretion of BTH_II1883 was completely abrogated in a mutant (Δ*4clpV*) lacking the *clpV* genes of the four T6SSs (T6SS-1, T6SS-2, T6SS-4, and T6SS-6) in *B. thailandensis* (Fig. 3*A*). Although complementation of the Δ*clpV4* (Fig. 3*A*) or Δ4*clpV* mutant (Fig. S4*A*) with *clpV4* restored BTH_II1883 secretion to the wild-type level, complementation of the Δ4*clpV* mutant with *clpV1*, *clpV2*, or *clpV6* has only minor effects on recovery of BTH_II1883 secretion (Fig. S4*A*). These data suggest that BTH_II1883 is a substrate primarily secreted by T6SS-4 although there might be substrate cross-recognition among different T6SSs. The T6SS-4 cluster has two *vgrG* genes encoding VgrG4a and VgrG4b. Similarly, the Δ*vgrG4a*Δ*vgrG4b* double mutant exhibited largely attenuated BTH_II1883 secretion, and complementation of either *vgrG4a* or *vgrG4b* partially restored BTH_II1883 secretion, indicating that the two VgrGs may act cooperatively as carriers in facilitation of TseM secretion (39) (Fig. S4*B*). In addition, TseM secretion was also impaired in the deletion mutant of *icmF4*, encoding a key T6SS structural protein, and restored in the complemented strain (Fig. S4*C*), further supporting that TseM secretion is mediated by the T6SS-4.

Analysis with atomic absorption spectrometry revealed that BTH_II1883 can specifically bind Mn^{2+} (Fig. 3*B*), and a binding K_d of 2.87 ± 0.32 μM was obtained by isothermal titration calorimetry (ITC) analysis (Fig. 3*C*, *Upper*). In addition, BTH_II1883 was not able to bind Ca^{2+}, Mg^{2+}, Zn^{2+}, and Fe^{3+} (Fig. 3*B*). The inability of BTH_II1883 to bind iron and zinc ions was also confirmed using the potassium ferricyanide assay (Fig. S5*A*) and the 4-(2-pyridylazo) resorcinol (PAR) assay, respectively (Fig. S5*B*). Thus, this protein is named type VI secretion system effector for Mn^{2+} binding (TseM). TseM is conserved in multiple *Burkholderia* species such as *B. pseudomallei*, *Burkholderia mallei*, and *Burkholderia oklahomensis* (Fig. S3*B*). Three dimensional structure simulation predicted several ion-binding residues (Gln35, His63, and Asp132) in TseM (Fig. S3*C*). Mutation of Gln35, His63, and Asn132 ($TseM^{Q35R/H63A/N132R}$) dramatically reduced (K_d = 219.4 ± 11.5 μM) but did not completely abrogate its affinity to Mn^{2+} (Fig. 3*C*, *Lower*), indicating the existence of other sites involved in Mn^{2+} binding.

Because of the Mn^{2+}-dependent T6SS-4 protection in oxidative stress resistance and the Mn^{2+} binding of TseM, we hypothesized that TseM is important for oxidative stress resistance. Indeed, in the presence of exogenous Mn^{2+} (0.25 μM), the Δ*tseM* mutant exhibited increased sensitivity to CHP treatment (Fig. 3*D*), elevated ROS levels (Fig. 3*E*), and reduced intracellular Mn^{2+} (Fig. 3*F*), resembling the T6SS-4 mutants. Complementation of *tseM* restores these phenotypes to wild-type levels (Fig. 3 *D*–*F*). Similar to T6SS-4 component genes, the expression of *tseM* was repressed by exogenous Mn^{2+} in a dose-dependent manner (Fig. 3*G*) and was induced by low Mn^{2+} (0.05 μM and 0.2 μM) under oxidative stress (Fig. S6*A*).

Next, we determined whether exogenous purified TseM restores the ability of relevant *B. thailandensis* mutants to survive oxidative challenge. Inclusion of metal-free TseM (1 μM) in cultures of the Δ*tseM* mutant fully restored its resistance to CHP, whereas inclusion of the Mn^{2+} binding attenuated the TseM* variant ($TseM^{Q35R/H63A/N132R}$), or complementation of the *tseM** (*tseM*$^{Q35R/H63A/N132R}$) gene only slightly recovered its resistance (Fig. 3*H*). Moreover, exogenously provided TseM protein, but not TseM protein, intracellularly produced by providing a plasmid encoding TseM, also protected the T6SS-4 mutant Δ*clpV4* from CHP-induced toxicity (Fig. 3*H*). This finding suggests that, after T6SS-4–mediated translocation, Mn^{2+} uptake by TseM occurred independently of the secretion system. Altogether, these data indicate that the Mn^{2+}-binding effector TseM is required for T6SS-4–dependent Mn^{2+} acquisition under oxidative stress.

TseM Interacts with a Mn^{2+}-Specific TonB-Dependent Outer Membrane Transporter. To reveal how TseM transports Mn^{2+} into the cell, we first attempted to identify bacterial components that interact with TseM. A GST pull-down assay was performed by incubating GST-Bind beads coated with GST-TseM or GST with cell lysates and supernatants of *B. thailandensis* wild type treated with CHP. After washing with PBS, proteins retained on the beads were resolved by sodium dodecyl sulfate polyacrylamide gel electrophoresis (SDS/PAGE) and then visualized by silver staining. Several proteins in the cell lysate with molecular weights ranging from 40 to 100 kDa were specifically retained by beads coated with GST-TseM, but not by beads coated with GST (Fig. 4*A*). Mass spectrometry analysis identified the 85-kDa band as a member of the TBDT (BTH_I1598); the 60-kDa band was the ATP-dependent RNA helicase DbpA (BTH_II0214); the band around 50 kDa was identified as a chaperone protein (BTH_I2937); and the band around 44 kDa was an iron complex transport system permease (BTH_II2142) (Fig. 4*A*).

The identification of a TonB-dependent outer membrane transporter prompted us to hypothesize that TseM engages receptor proteins on the bacterial surface to deliver Mn^{2+} into the cell. Indeed, the specific interaction between TseM and BTH_I1598 was confirmed by an in vitro binding assay with purified GST-BTH_I1598 and His_6-TseM proteins (Fig. 4*B*). Sequence analysis of BTH_I1598 predicted a 114-residue-long N-terminal TonB-plug domain (residues 68–181) and a TonB-dependent receptor domain from residue 529 to the C terminus of the protein (Fig. S7*A*). TBDTs are bacterial outer membrane transporters that mediate the active uptake of iron siderophores, vitamin B12, nickel, and zinc (40–42). According to phylogenetic tree analysis, BTH_I1598 formed an independent cluster evolutionarily distant from the known outer membrane zinc transporter ZnuD of *Neisseria meningitidis* (43) and nickel transporter FrpB4 in *Helicobacter mustelae* (44) (Fig. S7*B*). This result suggests that BTH_I1598 may be involved in transportation of other metal ions such as Mn^{2+}.

To test the role of BTH_I1598 in Mn^{2+} transport, we measured the total metal content of bacterial cells using ICP-MS. Our results revealed that deletion of BTH_I1598 significantly reduced intracellular Mn^{2+} levels compared with those of the wild type, and complementation of the gene restored to wild-type levels (Fig. 4*C*). By contrast, deletion of the *bth_I1598* gene had little effect on the accumulation of Fe and Zn ions (Fig. S5*C*). Consistent with its specific role in Mn^{2+} transport, the expression of BTH_I1598 was induced by low, but repressed by high, extracellular Mn^{2+} (Fig. 4*D* and Fig. S6*B*). Thus, we designated it Mn^{2+}-specific outer membrane transporter (MnoT).

Interestingly, similar to the T6SS-4 genes, the expression of *mnoT* was repressed by OxyR in our transcriptomic analysis (Dataset S1), and the repression by OxyR was confirmed by qRT-PCR analysis (Fig. 4*E*). The expression of *mnoT* was also induced by CHP (Fig. 4*D*). Thus, MnoT might be involved in the oxidative stress response in *B. thailandensis*. Indeed, the Δ*mnoT* mutant exhibited higher sensitivity to CHP than the wild-type and the complemented strain (Fig. 4*F*). Importantly, although exogenous Mn^{2+} (0.25 μM) enhanced the survival rate of the wild-type and complemented strain upon CHP challenge, the effect of exogenous Mn^{2+} was largely abolished in the Δ*mnoT* mutant (Fig. 4*F*). Similar results were obtained by comparing the growth of the *B. thailandensis* wild-type, the Δ*mnoT* mutant, and the complemented strain in the presence of EDTA under CHP stress (Fig. S2 *C* and *D*). These results suggest that MnoT is an outer membrane active Mn^{2+} transporter and important in oxidative stress resistance.

The Mn^{2+} Transport Activity of T6SS is MnoT Dependent. To investigate whether MnoT mediates the Mn^{2+} transport activity of TseM and T6SS-4, we constructed Δ*mnoT*Δ*tseM* and Δ*mnoT*Δ*clpV4* double mutants. Both mutants showed highly reduced survival under CHP challenge compared with the wild type (Fig. 5*A*). Complementation of the *tseM* gene completely rescued the sensitivity of the Δ*tseM* mutant to CHP (Fig. 3*D*) but had marginal effect on rescue of the sensitivity of the Δ*mnoT*Δ*tseM* double mutant (Fig. 5*A*). Moreover,

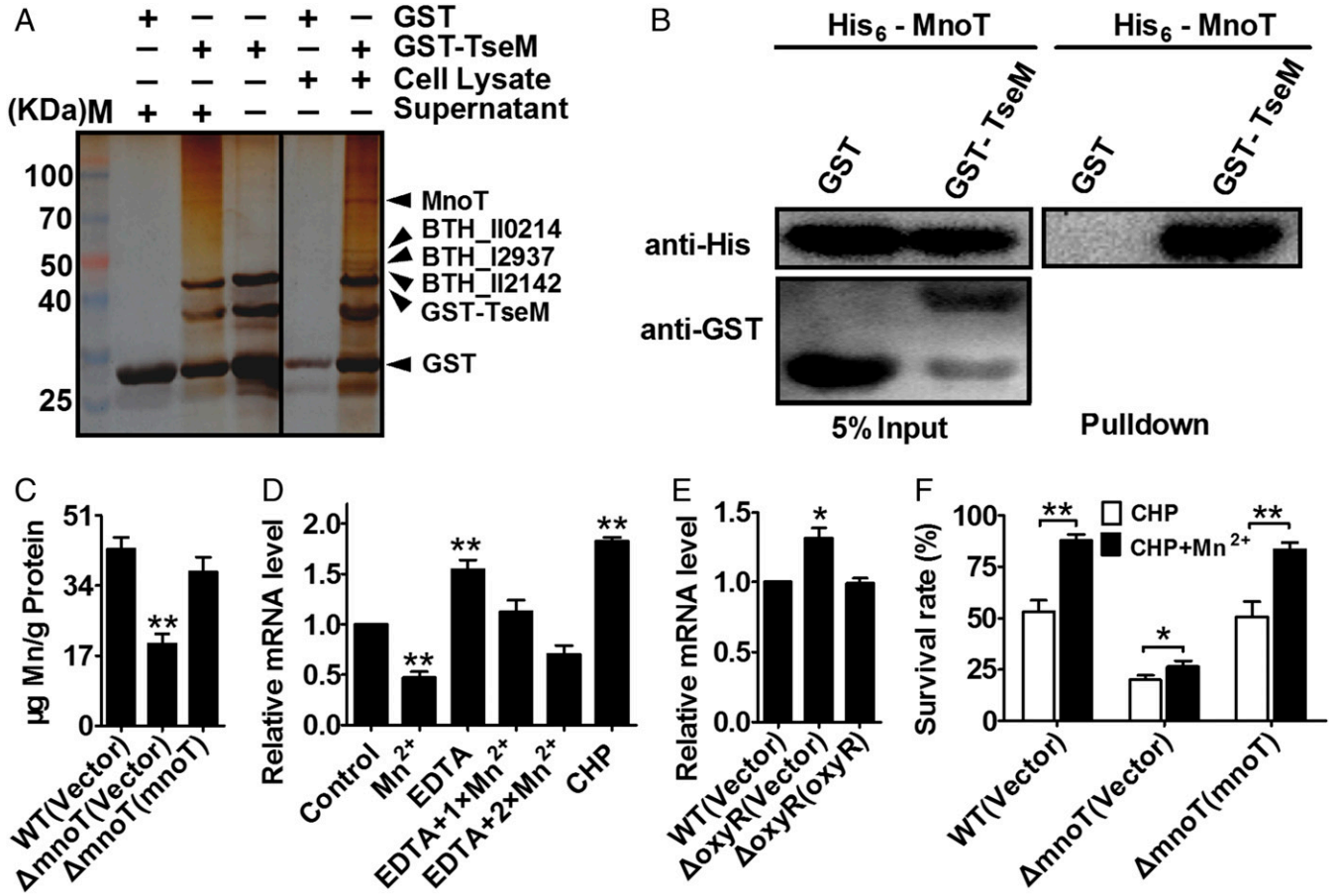

Fig. 4. TseM interacts with a TBDT family transporter involved in Mn^{2+} transport. (*A*) MnoT was retained by agarose beads coated with GST-TseM. GST-Bind beads coated with GST-TseM (lanes 2, 3, and 5) or GST (lanes 1 and 4) were incubated with CHP-treated *B. thailandensis* supernatant (lanes 1 and 2) or cell lysates (lanes 4 and 5). After washing with PBS, the proteins resolved by SDS/PAGE were visualized using silver staining, and bands that specifically retained by the GST-TseM–coated beads were identified by mass spectrometry. (*B*) Direct binding of TseM to MnoT. His_6-MnoT was incubated with GST-TseM or GST, and the protein complexes captured with glutathione beads were detected by Western blotting. (*C*) MnoT is involved in Mn^{2+} acquisition in *B. thailandensis*. Stationary phase *B. thailandensis* strains were exposed to 0.25 mM CHP for 20 min in PBS containing 0.25 μM $MnSO_4$. Mn^{2+} associated with bacterial cells was determined by ICP-MS. Data shown are the average and SD from three independent experiments. (*D*) MnoT expression was inhibited by high Mn^{2+} conditions and induced by CHP and EDTA. Cells of *B. thailandensis* wild type were grown in LB medium with 100 μM Mn^{2+}, 100 μM CHP, 100 μM EDTA, or 100 μM EDTA together with 100 μM Mn^{2+} (EDTA + 1× Mn^{2+}), and 100 μM EDTA together with 200 μM Mn^{2+} (EDTA + 2× Mn^{2+}). The expression of *mnoT* was measured by qRT-PCR. Data shown are the average and SD from three independent experiments. $^{**}P \leq 0.01$; $^{*}P \leq 0.05$. (*E*) The expression of MnoT was negatively regulated by OxyR. Cells of relevant *B. thailandensis* strains were grown in LB medium and the expression of *mnoT* was measured by qRT-PCR. Data shown are the average and SD from three independent experiments. (*F*) Alleviation of the sensitivity of *B. thailandensis* strains to CHP by exogenous Mn^{2+} (0.25 μM) required MnoT. The viability of relevant stationary *B. thailandensis* strains was determined after exposure to CHP or CHP with 0.25 μM Mn^{2+} for 40 min. The mean values and SD from at least three repeats are shown. $^{**}P \leq 0.01$; $^{*}P \leq 0.05$.

although exogenous addition of metal-free apo-TseM (1 μM) significantly increased the survival of both the wild type and the Δ*tseM* mutant under CHP challenge (Fig. 3*H*), this effect was completely abolished in the Δ*mnoT*Δ*tseM*(*vector*) and Δ*mnoT*Δ*tseM*(*tseM*) strains (Fig. 5*A*). However, exogenous TseM protein efficiently protected the Δ*mnoT*Δ*tseM* mutant from CHP toxicity when the *mnoT* gene was complemented (Fig. 5*A*). Similarly, complementation of *clpV4* failed to rescue the sensitivity of the Δ*mnoT*Δ*clpV4* double mutant to CHP, and exogenous apo-TseM protected Δ*mnoT*Δ*clpV4*(*mnoT*) but not Δ*mnoT*Δ*clpV4* (*vector*) or Δ*mnoT*Δ*clpV4*(*clpV4*) from CHP toxicity (Fig. 5*A*). These results demonstrate that the antioxidant activity and related Mn^{2+} transport activity of T6SS-4 and TseM are mediated by MnoT.

To reveal more about the mechanisms of Mn^{2+} transport mediated by MnoT and T6SS-4, we performed intrabacterial growth competition assays between different *B. thailandensis* strains under CHP challenge in liquid M9 medium containing 25 nM Mn^{2+}. As shown in Fig. 5*B*, the wild type displayed a growth advantage when competing with Δ*mnoT* but not Δ*tseM* and Δ*clpV4*. Indeed, the Δ*mnoT* mutant displayed a 2.5- to 3.5-fold growth disadvantage when competing with not only the wild type, but also the Δ*tseM* and Δ*clpV4* mutants. However, introducing the Δ*mnoT* mutation to the Δ*tseM* or the Δ*clpV4* mutants abolished their competitive advantage over the Δ*mnoT* mutant. This result suggests that MnoT can indiscriminately transport Mn^{2+}-bound TseM secreted by itself or other neighboring cells.

The importance of MnoT in mediation of the Mn^{2+} transport activity of T6SS-4 was further confirmed by interbacterial growth competition assays between *B. thailandensis* strains and *Escherichia coli* K12. Phylogenetic analysis shows that, whereas MnoT homologs are widely distributed in *Burkholderia* species, it is absent in *E. coli* K12 (Fig. S8). As shown in Fig. 5*C*, the *B. thailandensis* wild type was highly competitive against the *E. coli* K12 competitor under 50 μM CHP challenge in liquid M9 medium containing 25 nM Mn^{2+}. However, the competitive advantage of *B. thailandensis* wild type over *E. coli* K12 was largely abolished in the Δ*tseM*, Δ*clpV4*, and

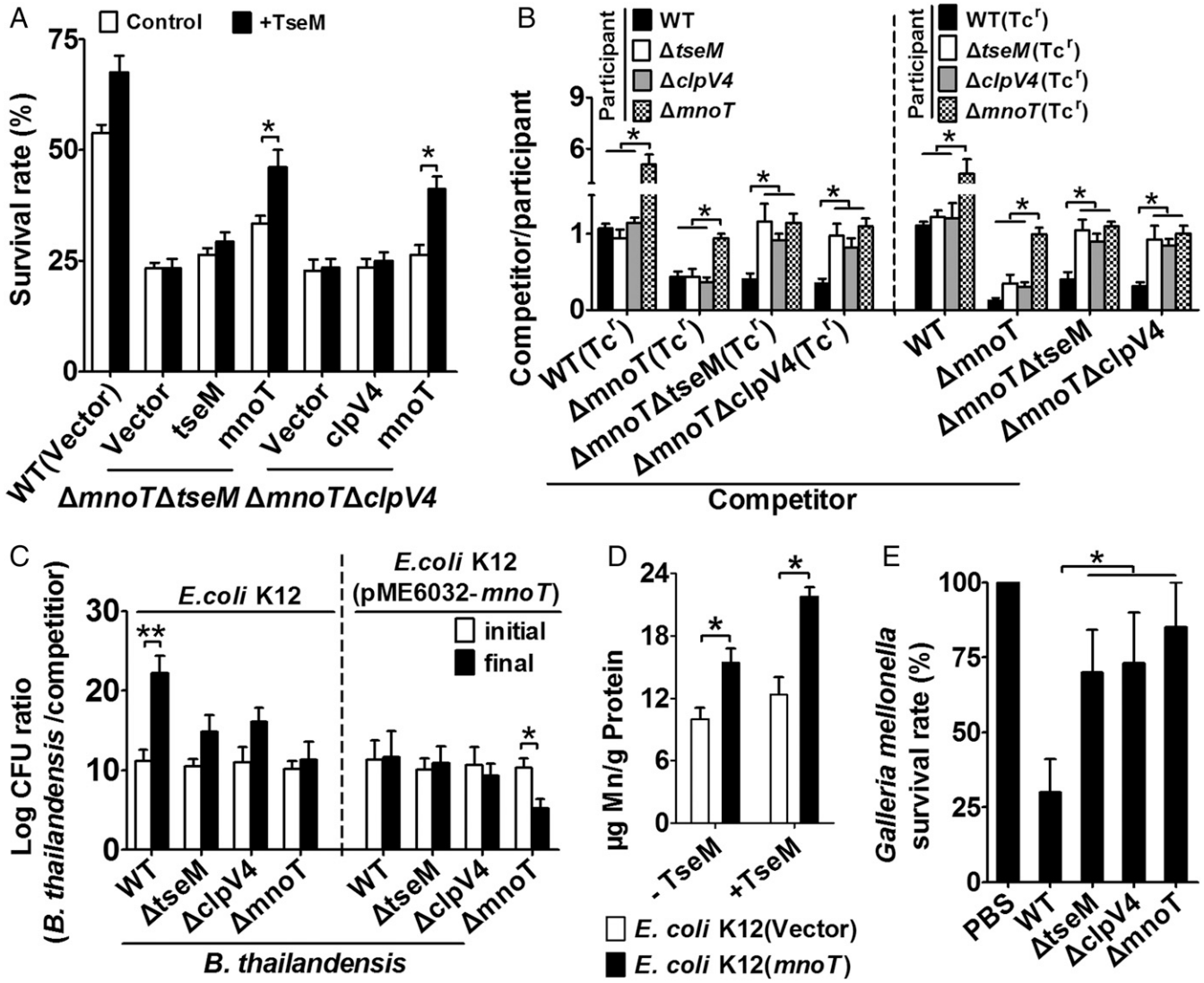

Fig. 5. The Mn^{2+} transport activity of TseM is dependent on MnoT. (*A*) The indicated bacterial strains grown to the stationary phase were exposed to CHP (0.25 mM) for 40 min in M9 medium containing 25 nM Mn^{2+}, and the viability of the cells was determined. (*B*) Intrabacterial growth competition assays between the indicated competitor strains (*x*-axis) following incubation with participant strains at 37 °C for 12 h in M9 medium containing 20 μM CHP. The competitive index result is calculated as the final cfu ratio (competitor/participant) divided by the initial ratio. (*C*) Interbacterial growth competition assays between *B. thailandensis* and *E. coli* K12. Quantification of cfu before (initial) and after (final) growth competition assays between the indicated organisms. The cfu ratio of the relevant *B. thailandensis* strains versus the competitors is plotted. (*D*) MnoT enhanced Mn^{2+} accumulation in *E. coli* K12. Stationary phase *E. coli* K12(pME6032) and *E. coli* K12(pME6032-*mnoT*) strains were cultivated in M9 medium containing 50 μM CHP, 25 nM Mn^{2+}, with (+) or without (–) 1 μM TseM, and intracellular Mn^{2+} was measured by ICP-MS. (*E*) Virulence survival of relative *B. thailandensis* strains in *G. mellonella* larvae. Ordinate represented the mean percentage survival rate of *G. mellonella* infected with different strains after 16 h. Error bars represent the SD from three independent experiments. $^{**}P \leq 0.01$; $^{*}P \leq 0.05$.

Δ*mnoT* mutants (Fig. 5*C*). As a TonB-dependent outer membrane transporter, we reasoned that heterologous expression of MnoT in *E. coli* K12 will improve its capability in Mn^{2+} acquisition and growth fitness. As expected, expression of MnoT increased intracellular Mn^{2+} accumulation in *E. coli* K12 under oxidative stress condition especially in the presence of exogenously provided TseM protein (Fig. 5*D*). Moreover, expression of MnoT abrogated the competition advantage of the *B. thailandensis* wild type to the *E. coli* K12 competitor (Fig. 5*C*). In addition, whereas the *E. coli* K12 (pME6032-*mnoT*) competitor showed equivalent competitive ability to the *B. thailandensis* Δ*tseM* and Δ*clpV4* mutants, it outcompeted the *B. thailandensis* Δ*mnoT* mutant (Fig. 5*C*). Altogether, these data indicate the essential role of MnoT for the T6SS-4–dependent Mn^{2+} uptake that confers a contact-independent competitive advantage.

***B. thailandensis* Mutants Lacking *clpV4*, *tseM*, or *mnoT* Are Defective in Virulence in the *Galleria mellonella* Larvae Infection Model.** Mn^{2+} uptake systems have been reported to be required for full virulence of multiple bacterial pathogens (2, 7). To investigate the role of T6SS-4-dependent Mn^{2+} transport system in pathogenesis, *G. mellonella* (wax moth) larvae were infected with different *B. thailandensis* strains to determine their abilities to kill the larvae. The *G. mellonella* larvae infection model has been widely used to assess the virulence of various Gram-negative and Gram-positive bacterial species (45, 46). Infection with *B. thailandensis* wild type exhibited the lowest survival rate at an average of 27%, whereas challenge with mutants lacking *clpV4*, *tseM*, or *mnoT* resulted in the mean survival rates of ∼70%, 73%, and 85% of larvae, respectively (Fig. 5*E*). These data suggest that the T6SS-4–dependent Mn^{2+} transport system is important for virulence.

Discussion

Although metal ions can traverse across the outer membrane via passive diffusion, Gram-negative bacteria must effectively concentrate scarce metal ions into the cytosol via active transport systems to meet cellular demands (47). To date, no active transporter for the translocation of Mn^{2+} across the outer membrane has been described. Here we propose a model of active transport of Mn^{2+} across the outer membrane mediated by the TonB-dependent outer membrane transporter MnoT and the T6SS effector TseM. Under high Mn^{2+} conditions, passive diffusion of Mn^{2+} through porins such as MnoP followed by transport across the inner membrane via either MntH or SitABCD fulfills cellular Mn^{2+} requirements. Low Mn^{2+} triggers the induction of the TonB-dependent outer membrane transporter MnoT for the active transport of Mn^{2+} across the outer membrane. When the bacterium encounters an oxidative stress challenge, T6SS-4 is induced to secrete the TseM manganeseophore into the extracellular milieu. Secreted TseM scavenges extracellular Mn^{2+} and delivers its Mn^{2+} load via direct interaction with MnoT. This active transport of Mn^{2+}, mediated by TseM and MnoT, fulfills the increased cellular demand for Mn^{2+} under oxidative stress (Fig. 6). This T6SS-mediated Mn^{2+} uptake model not only expands our current understanding of the diverse T6SS functions but also provides insights for the interaction between specialized protein secretion systems and metal acquisition.

Several lines of evidence indicate that MnoT functions in Mn^{2+} uptake. First, the Δ*mnoT* mutant was strongly deficient in Mn^{2+} accumulation under Mn^{2+} limitation (Fig. 4*C*). Next, MnoT was necessary to support bacterial growth under Mn^{2+}-limited and oxidative stress conditions (Fig. S2 *C* and *D*). Moreover, deletion of *mnoT* abolished the protective effect of exogenous Mn^{2+} on oxidative stress resistance (Fig. 4*F*). Finally, as a Mn^{2+} transporter, the expression of *mnoT* was induced by low concentrations but repressed by high concentrations of Mn^{2+} (Fig. 4*D* and Fig. S6*B*). Consistent with its role in oxidative stress resistance, the expression of *mnoT* was also controlled by OxyR (Fig. 4*E*). These results indicate that *mnoT* encodes a novel Mn^{2+} uptake system that facilitates the uptake of Mn^{2+} at low concentrations and plays a crucial role in resistance to oxidative stress. To the best of our knowledge, an active transporter for translocation of Mn^{2+} across the outer membrane has not been previously described.

Most TBDTs studied to date are involved in the acquisition of iron by means of siderophore substrates (42, 48, 49). The siderophore substrates range in complexity from simple small molecules such as citrates to large proteins such as hemophores (48, 50). Bacterial hemophores are secreted proteins that scavenge heme in the external medium and bring it back to their specific outer membrane receptors (51, 52). Although proteinaceous metallophores such as nickelophore and zincophore have been proposed to be involved in TBDT-mediated nickel and zinc transport, none of these has been experimentally verified (43, 44). In the present study, we provide the following evidence that TseM facilitates MnoT-mediated Mn^{2+} transport under oxidative stress by acting as a manganeseophore: (*i*) recombinant TseM exhibited Mn^{2+} binding capacity (Fig. 3 *B* and *C*); (*ii*) the *tseM* mutant was strongly deficient in Mn^{2+} accumulation under oxidative stress conditions (Fig. 3*F*); (*iii*) deletion of *tseM* dramatically abolished the effect of exogenous Mn^{2+} on oxidative stress resistance (Fig. 3 *D* and *E*); (*iv*) the expression of *tseM* was repressed by high concentrations of Mn^{2+} (Fig. 3*G*); (*v*) TseM directly interacts with MnoT (Fig. 4 *A* and *B*); and (*vi*) the function of TseM on Mn^{2+} transport and oxidative stress resistance is highly dependent on the presence of MnoT (Fig. 5 *A*–*D*). We thus tentatively suggest the term "manganeseophore" for secreted Mn^{2+} binding proteins, which sequester this metal from the environment and interact with the outer membrane transporter for improved Mn^{2+} uptake.

We present TseM as a description of a proteinaceous metallophore other than hemophores for scavenging heme iron. Indeed, the TseM–MnoT manganese transport system shares some functional similarities with the bacterial HasA hemophore system. In the HasA system, the heme-binding protein HasA secreted by the type I secretion system scavenges heme from the host and presents it to a specific TBDT outer membrane transporter, HasR, whereby it is internalized by a TonB-dependent process (51, 52). Similarly, the T6SS secreted TseM scavenges manganese in the extracellular medium and reassociates with the TBDT transporter, MnoT, to facilitate bacterial manganese acquisition. Whether such

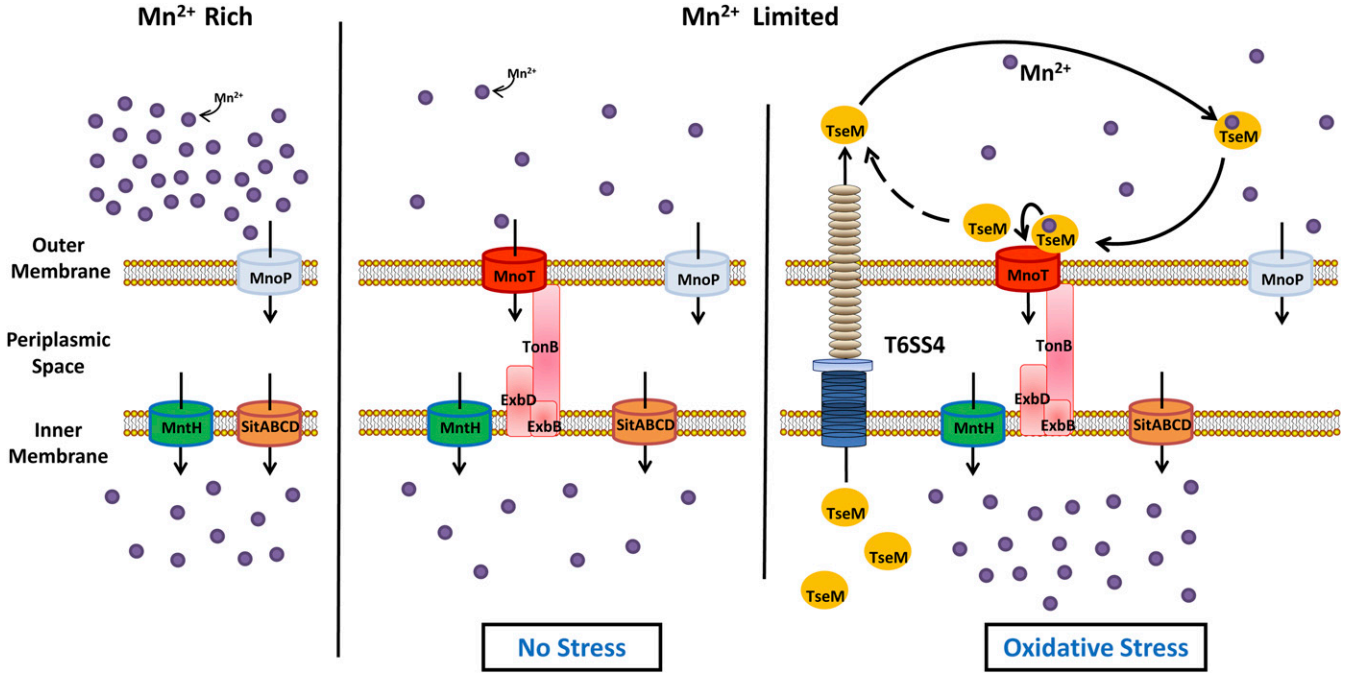

Fig. 6. Model of T6SS-4–mediated Mn^{2+} transport and oxidative resistance in *B. thailandensis*.

metallophore–TBDT systems exist for the transport of other metal ions such as zinc and nickel require further investigation.

Together with the report that T6SS is involved in Zn^{2+} uptake in *Y. pseudotuberculosis* (32), our finding of the involvement of T6SS in Mn^{2+} uptake significantly expands the range of known functions of this specialized protein secretion system. Recently, Chen et al. (53) reported that the T6SS in *Pseudomonas taiwanensis* is involved in the secretion of iron chelator pyoverdine. Although the secretion mechanism of pyoverdine remains unidentified, this study implies the role of T6SS in iron uptake. Moreover, previous reports have shown that the expression of some T6SSs was regulated by iron and zinc in *B. mallei* and *B. pseudomallei* (35), and by the ferric uptake regulator Fur in *Pseudomonas aeruginosa* (54), further supporting the role of T6SS in metal ion acquisition. Therefore, we postulate that the "metal transporting" T6SSs may represent a novel type of T6SS that secretes metal scavenging proteins into the extracellular milieu for transport of various metal ions.

Antibacterial activities of the T6SS can induce ROS generation in target cells, which contribute to target cell death (55). In contrast, the metal transporting T6SSs can reduce intracellular ROS levels by taking up antioxidative Mn^{2+} (Fig. 2) and Zn^{2+} (32). Indeed, the *B. thailandensis* T6SS-4 reported here conferred bacteria a contact-independent competitive advantage in both interspecies and intraspecies bacterial competition (Fig. 5 *B* and *C*) through transporting Mn^{2+} under oxidative stress conditions, which is distinct from the contact-dependent competitive advantage conferred by those well-described antibacterial T6SSs (22, 24, 56). Thus, T6SSs play crucial roles in shaping the composition of a microbial population in the host or environmental niche, either by direct killing of competing cells via contact-dependent translocation of toxins, or by competition for essential nutrients via contact-independent secretion of proteinaceous metallophore. It will be interesting to investigate whether the metal transporting T6SS can puncture and inject toxins into target cells, or whether somehow this system has lost any puncturing ability of target cells and has been redesigned exclusively for extracellular release.

Because manganese is an essential micronutrient for bacterial growth, bacterial pathogens have evolved efficient mechanisms to acquire Mn^{2+} from the nutrient-restricted host environment to cause disease (2, 7). Indeed, Mn^{2+} uptake systems were reported to be required for full virulence of multiple bacterial pathogens such as *Yersinia pestis* (57), *Y. pseudotuberculosis* (13), *Streptococcus mutans* (58), *Salmonella enterica* serovar Typhimurium (59), *Borrelia burgdorferi* (60), and *Brucella abortus* (61) in different animal models. Consistently, we found the *B. thailandensis* Δ*mnoT*, Δ*tseM*, and Δ*clpV4* mutants were attenuated in virulence in the *G. mellonella* larvae infection model (Fig. 5*E*), suggesting the importance of the T6SS-4–mediated Mn^{2+} transport system in the resistance to host nutritional immunity. Similar results were reported for the T6SS involved in Zn^{2+} uptake in *Y. pseudotuberculosis* in a mouse infection model (32). Thus, the metal transporting T6SSs may represent a promising target for therapeutic development of new antimicrobials.

Materials and Methods

Bacterial Strains and Growth Conditions. Bacterial strains, plasmids, and primers used in this study are listed in Dataset S2. *E. coli* and *B. thailandensis* strains were cultured in LB aerobically on a rotary shaker (220 rpm) or on LB plates at 37 °C. The *B. thailandensis* E264 strain was the parent of all derivatives used in this study (62). M9 medium containing different levels of Mn^{2+} was used for survival assay and bacterial competition assay.

Protein Secretion Assay. Secretion assays for TseM (BTH_II1883) were performed according to described methods (63). Briefly, strains were inoculated into 200 mL LB and incubated with continuous shaking until OD_{600} reached 1.6 at 37 °C. A 2-mL culture was centrifuged and the cell pellet was resuspended in 100 μL SDS-loading buffer; this whole-cell lysate sample was defined as $TseM_{IN}$. A total of 180 mL of the culture was centrifuged, and the supernatant was filtered through a 0.22-μm filter (Millipore) and secreted proteins in the supernatant were collected by filtration over a nitrocellulose filter (BA85) (Whatman) three times. The filter was soaked in 100 μL SDS sample buffer for 15 min at 65 °C to recover the proteins present, and the sample was defined as $TseM_{OUT}$. All samples were normalized to the OD_{600} of the culture and volume used in preparation.

Detailed protocols for these experiments and additional procedures are described in detail in *SI Materials and Methods*.

ACKNOWLEDGMENTS. We thank Professor Zhao-Qing Luo (Purdue University) for valuable discussions and critical reading of the manuscript and Professor Feng Shao and Dr. Qiuhe Lu (National Institute of Biological Sciences, Beijing) for kindly providing strains and plasmids. This work was supported by the National Natural Science Foundation of China (Grants 31670053, 31370150, and 31500087) and Fundamental Research Funds for the Central Universities, Northwest A&F University (Grant 2452015100). T.G.D. was supported by a Government of Canada Research Chair award and Canadian Foundation for Innovation Grant CFI-JELF. B.B. was supported by an Alberta Innovates Health Solutions postdoctoral fellowship and a Canadian Natural Sciences and Engineering Research Council fellowship.

1. Aguirre JD, Culotta VC (2012) Battles with iron: Manganese in oxidative stress protection. *J Biol Chem* 287(17):13541–13548.
2. Lisher JP, Giedroc DP (2013) Manganese acquisition and homeostasis at the host-pathogen interface. *Front Cell Infect Microbiol* 3:91.
3. Anjem A, Varghese S, Imlay JA (2009) Manganese import is a key element of the OxyR response to hydrogen peroxide in *Escherichia coli*. *Mol Microbiol* 72(4):844–858.
4. Barnese K, Gralla EB, Valentine JS, Cabelli DE (2012) Biologically relevant mechanism for catalytic superoxide removal by simple manganese compounds. *Proc Natl Acad Sci USA* 109(18):6892–6897.
5. Puri S, Hohle TH, O'Brian MR (2010) Control of bacterial iron homeostasis by manganese. *Proc Natl Acad Sci USA* 107(23):10691–10695.
6. Hood MI, Skaar EP (2012) Nutritional immunity: Transition metals at the pathogen-host interface. *Nat Rev Microbiol* 10(8):525–537.
7. Juttukonda LJ, Skaar EP (2015) Manganese homeostasis and utilization in pathogenic bacteria. *Mol Microbiol* 97(2):216–228.
8. Diaz-Ochoa VE, et al. (2016) *Salmonella* mitigates oxidative stress and thrives in the inflamed gut by evading calprotectin-mediated manganese sequestration. *Cell Host Microbe* 19(6):814–825.
9. Kehres DG, Janakiraman A, Slauch JM, Maguire ME (2002) SitABCD is the alkaline $Mn^{(2+)}$ transporter of *Salmonella enterica* serovar Typhimurium. *J Bacteriol* 184(12):3159–3166.
10. Sabri M, et al. (2008) Contribution of the SitABCD, MntH, and FeoB metal transporters to the virulence of avian pathogenic *Escherichia coli* O78 strain χ7122. *Infect Immun* 76(2):601–611.
11. Kehres DG, Zaharik ML, Finlay BB, Maguire ME (2000) The NRAMP proteins of *Salmonella typhimurium* and *Escherichia coli* are selective manganese transporters involved in the response to reactive oxygen. *Mol Microbiol* 36(5):1085–1100.
12. Patzer SI, Hantke K (2001) Dual repression by $Fe^{(2+)}$-Fur and $Mn^{(2+)}$-MntR of the *mntH* gene, encoding an NRAMP-like $Mn^{(2+)}$ transporter in *Escherichia coli*. *J Bacteriol* 183(16):4806–4813.
13. Champion OL, et al. (2011) *Yersinia pseudotuberculosis mntH* functions in intracellular manganese accumulation, which is essential for virulence and survival in cells expressing functional Nramp1. *Microbiology* 157(Pt 4):1115–1122.
14. Hohle TH, Franck WL, Stacey G, O'Brian MR (2011) Bacterial outer membrane channel for divalent metal ion acquisition. *Proc Natl Acad Sci USA* 108(37):15390–15395.
15. Durand E, Cambillau C, Cascales E, Journet L (2014) VgrG, Tae, Tle, and beyond: The versatile arsenal of Type VI secretion effectors. *Trends Microbiol* 22(9):498–507.
16. Russell AB, Peterson SB, Mougous JD (2014) Type VI secretion system effectors: Poisons with a purpose. *Nat Rev Microbiol* 12(2):137–148.
17. Ho BT, Dong TG, Mekalanos JJ (2014) A view to a kill: The bacterial type VI secretion system. *Cell Host Microbe* 15(1):9–21.
18. Basler M (2015) Type VI secretion system: Secretion by a contractile nanomachine. *Philos Trans R Soc Lond B Biol Sci* 370(1679).
19. Cascales E (2008) The type VI secretion toolkit. *EMBO Rep* 9(8):735–741.
20. Pukatzki S, McAuley SB, Miyata ST (2009) The type VI secretion system: Translocation of effectors and effector-domains. *Curr Opin Microbiol* 12(1):11–17.
21. Hood RD, et al. (2010) A type VI secretion system of *Pseudomonas aeruginosa* targets a toxin to bacteria. *Cell Host Microbe* 7(1):25–37.
22. Schwarz S, et al. (2010) Burkholderia type VI secretion systems have distinct roles in eukaryotic and bacterial cell interactions. *PLoS Pathog* 6(8):e1001068.
23. Zhang W, et al. (2013) A type VI secretion system regulated by OmpR in *Yersinia pseudotuberculosis* functions to maintain intracellular pH homeostasis. *Environ Microbiol* 15(2):557–569.
24. Russell AB, et al. (2011) Type VI secretion delivers bacteriolytic effectors to target cells. *Nature* 475(7356):343–347.
25. Russell AB, et al. (2013) Diverse type VI secretion phospholipases are functionally plastic antibacterial effectors. *Nature* 496(7446):508–512.
26. Dong TG, Ho BT, Yoder-Himes DR, Mekalanos JJ (2013) Identification of T6SS-dependent effector and immunity proteins by Tn-seq in *Vibrio cholerae*. *Proc Natl Acad Sci USA* 110(7):2623–2628.

27. Ma LS, Hachani A, Lin JS, Filloux A, Lai EM (2014) *Agrobacterium tumefaciens* deploys a superfamily of type VI secretion DNase effectors as weapons for interbacterial competition in planta. *Cell Host Microbe* 16(1):94–104.
28. Aubert DF, et al. (2016) A Burkholderia type VI rffector feamidates Rho GTPases to activate the pyrin inflammasome and trigger inflammation. *Cell Host Microbe* 19(5): 664–674.
29. Jiang F, et al. (2016) The *Pseudomonas aeruginosa* type VI secretion PGAP1-like effector induces host autophagy by activating endoplasmic reticulum stress. *Cell Reports* 16(6):1502–1509.
30. Pukatzki S, Ma AT, Revel AT, Sturtevant D, Mekalanos JJ (2007) Type VI secretion system translocates a phage tail spike-like protein into target cells where it cross-links actin. *Proc Natl Acad Sci USA* 104(39):15508–15513.
31. Hachani A, Wood TE, Filloux A (2016) Type VI secretion and anti-host effectors. *Curr Opin Microbiol* 29:81–93.
32. Wang T, et al. (2015) Type VI secretion system transports Zn^{2+} to combat multiple stresses and host immunity. *PLoS Pathog* 11(7):e1005020.
33. Haraga A, West TE, Brittnacher MJ, Skerrett SJ, Miller SI (2008) *Burkholderia thailandensis* as a model system for the study of the virulence-associated type III secretion system of *Burkholderia pseudomallei*. *Infect Immun* 76(11):5402–5411.
34. Garcia EC, Perault AI, Marlatt SA, Cotter PA (2016) Interbacterial signaling via *Burkholderia* contact-dependent growth inhibition system proteins. *Proc Natl Acad Sci USA* 113(29):8296–8301.
35. Burtnick MN, Brett PJ (2013) *Burkholderia mallei* and *Burkholderia pseudomallei* cluster 1 type VI secretion system gene expression is negatively regulated by iron and zinc. *PLoS One* 8(10):e76767.
36. Loprasert S, Whangsuk W, Sallabhan R, Mongkolsuk S (2003) Regulation of the *katG-dpsA* operon and the importance of KatG in survival of *Burkholderia pseudomallei* exposed to oxidative stress. *FEBS Lett* 542(1–3):17–21.
37. Tseng HJ, McEwan AG, Apicella MA, Jennings MP (2003) OxyR acts as a repressor of catalase expression in *Neisseria gonorrhoeae*. *Infect Immun* 71(1):550–556.
38. Teramoto H, Inui M, Yukawa H (2013) OxyR acts as a transcriptional repressor of hydrogen peroxide-inducible antioxidant genes in *Corynebacterium glutamicum* R. *FEBS J* 280(14):3298–3312.
39. Hachani A, Allsopp LP, Oduko Y, Filloux A (2014) The VgrG proteins are "à la carte" delivery systems for bacterial type VI effectors. *J Biol Chem* 289(25):17872–17884.
40. Nikaido H (2003) Molecular basis of bacterial outer membrane permeability revisited. *Microbiol Mol Biol Rev* 67(4):593–656.
41. Ferguson AD, Deisenhofer J (2004) Metal import through microbial membranes. *Cell* 116(1):15–24.
42. Noinaj N, Guillier M, Barnard TJ, Buchanan SK (2010) TonB-dependent transporters: Regulation, structure, and function. *Annu Rev Microbiol* 64:43–60.
43. Stork M, et al. (2010) An outer membrane receptor of *Neisseria meningitidis* involved in zinc acquisition with vaccine potential. *PLoS Pathog* 6:e1000969.
44. Schauer K, Gouget B, Carrière M, Labigne A, de Reuse H (2007) Novel nickel transport mechanism across the bacterial outer membrane energized by the TonB/ExbB/ExbD machinery. *Mol Microbiol* 63(4):1054–1068.
45. Wand ME, Müller CM, Titball RW, Michell SL (2011) Macrophage and *Galleria mellonella* infection models reflect the virulence of naturally occurring isolates of *B. pseudomallei*, *B. thailandensis* and *B. oklahomensis*. *BMC Microbiol* 11(1):11.
46. Ramarao N, Nielsen-Leroux C, Lereclus D (2012) The insect *Galleria mellonella* as a powerful infection model to investigate bacterial pathogenesis. *J Vis Exp* 70(70): e4392.
47. Finney LA, O'Halloran TV (2003) Transition metal speciation in the cell: Insights from the chemistry of metal ion receptors. *Science* 300(5621):931–936.
48. Cassat JE, Skaar EP (2013) Iron in infection and immunity. *Cell Host Microbe* 13(5): 509–519.
49. Porcheron G, Garénaux A, Proulx J, Sabri M, Dozois CM (2013) Iron, copper, zinc, and manganese transport and regulation in pathogenic *Enterobacteria*: correlations between strains, site of infection and the relative importance of the different metal transport systems for virulence. *Front Cell Infect Microbiol* 3:90.
50. Maresso AW, Garufi G, Schneewind O (2008) *Bacillus anthracis* secretes proteins that mediate heme acquisition from hemoglobin. *PLoS Pathog* 4(8):e1000132.
51. Contreras H, Chim N, Credali A, Goulding CW (2014) Heme uptake in bacterial pathogens. *Curr Opin Chem Biol* 19:34–41.
52. Cescau S, et al. (2007) Heme acquisition by hemophores. *Biometals* 20(3–4):603–613.
53. Chen WJ, et al. (2016) Involvement of type VI secretion system in secretion of iron chelator pyoverdine in *Pseudomonas taiwanensis*. *Sci Rep* 6:32950.
54. Sana TG, et al. (2012) The second type VI secretion system of *Pseudomonas aeruginosa* strain PAO1 is regulated by quorum sensing and Fur and modulates internalization in epithelial cells. *J Biol Chem* 287(32):27095–27105.
55. Dong TG, et al. (2015) Generation of reactive oxygen species by lethal attacks from competing microbes. *Proc Natl Acad Sci USA* 112(7):2181–2186.
56. MacIntyre DL, Miyata ST, Kitaoka M, Pukatzki S (2010) The *Vibrio cholerae* type VI secretion system displays antimicrobial properties. *Proc Natl Acad Sci USA* 107(45): 19520–19524.
57. Perry RD, et al. (2012) Manganese transporters Yfe and MntH are Fur-regulated and important for the virulence of *Yersinia pestis*. *Microbiology* 158(Pt 3):804–815.
58. Paik S, Brown A, Munro CL, Cornelissen CN, Kitten T (2003) The *sloABCR* operon of *Streptococcus mutans* encodes an Mn and Fe transport system required for endocarditis virulence and its Mn-dependent repressor. *J Bacteriol* 185(20):5967–5975.
59. Boyer E, Bergevin I, Malo D, Gros P, Cellier MF (2002) Acquisition of Mn(II) in addition to Fe(II) is required for full virulence of *Salmonella enterica* serovar Typhimurium. *Infect Immun* 70(11):6032–6042.
60. Ouyang Z, He M, Oman T, Yang XF, Norgard MV (2009) A manganese transporter, BB0219 (BmtA), is required for virulence by the Lyme disease spirochete, *Borrelia burgdorferi*. *Proc Natl Acad Sci USA* 106(9):3449–3454.
61. Anderson ES, et al. (2009) The manganese transporter MntH is a critical virulence determinant for *Brucella abortus* 2308 in experimentally infected mice. *Infect Immun* 77(8):3466–3474.
62. Zhao Y, Shao F (2015) The NAIP-NLRC4 inflammasome in innate immune detection of bacterial flagellin and type III secretion apparatus. *Immunol Rev* 265(1):85–102.
63. Xu S, et al. (2014) FliS modulates FlgM activity by acting as a non-canonical chaperone to control late flagellar gene expression, motility and biofilm formation in *Yersinia pseudotuberculosis*. *Environ Microbiol* 16(4):1090–1104.
64. Xu L, et al. (2010) Inhibition of host vacuolar H^+-ATPase activity by a *Legionella pneumophila* effector. *PLoS Pathog* 6(3):e1000822.
65. Vogel A, Schilling O, Niecke M, Bettmer J, Meyer-Klaucke W (2002) ElaC encodes a novel binuclear zinc phosphodiesterase. *J Biol Chem* 277(32):29078–29085.
66. Schilling O, et al. (2005) Zinc- and iron-dependent cytosolic metallo-beta-lactamase domain proteins exhibit similar zinc-binding affinities, independent of an atypical glutamate at the metal-binding site. *Biochem J* 385(Pt 1):145–153.
67. Huang X, Kocabas E, Hernick M (2011) The activity and cofactor preferences of N-acetyl-1-D-myo-inosityl-2-amino-2-deoxy-α-D-glucopyranoside deacetylase (MshB) change depending on environmental conditions. *J Biol Chem* 286(23):20275–20282.
68. Hunt JB, Neece SH, Schachman HK, Ginsburg A (1984) Mercurial-promoted Zn2+ release from Escherichia coli aspartate transcarbamoylase. *J Biol Chem* 259(23): 14793–14803.
69. Saraswathi R, Pait Chowdhury R, Williams SM, Ghatak P, Chatterji D (2009) The mycobacterial MsDps2 protein is a nucleoid-forming DNA binding protein regulated by sigma factors sigma and sigma. *PLoS One* 4(11):e8017.
70. Jiang F, Waterfield NR, Yang J, Yang G, Jin Q (2014) A *Pseudomonas aeruginosa* type VI secretion phospholipase D effector targets both prokaryotic and eukaryotic cells. *Cell Host Microbe* 15(5):600–610.
71. Russell AB, et al. (2014) A type VI secretion-related pathway in Bacteroidetes mediates interbacterial antagonism. *Cell Host Microbe* 16(2):227–236.
72. Hisabori T, et al. (2005) Thioredoxin affinity chromatography: A useful method for further understanding the thioredoxin network. *J Exp Bot* 56(416):1463–1468.

Supporting Information

Si et al. 10.1073/pnas.1614902114

SI Materials and Methods

Antibiotics and Chemicals. All chemicals were of Analytical Reagent Grade purity or higher. Antibiotics were added at the following concentrations: Chloramphenicol, 34 μg·ml^{-1} for *E. coli* and 50 μg·ml^{-1} for *B. thailandensis*; kanamycin, 50 μg·ml^{-1} for *E. coli*; streptomycin, 100 μg·ml^{-1} for *B. thailandensis*; ampicillin, 100 μg·ml^{-1} for *E. coli*; tetracycline, 25 μg·ml^{-1} for *E. coli*, and 50 μg·ml^{-1} for *B. thailandensis*.

Plasmid Construction. For obtaining expression plasmids, the genes encoding *B. thailandensis* TseM (BTH_II1883), OxyR (BTH_I1281), and MnoT (BTH_I1598) were amplified by PCR. The obtained DNA fragments were digested and cloned into similar digested pGEX6p-1, pET28a, and pET15b, yielding corresponding plasmid derivatives. To prepare the Δ*clpV4* in-frame deletion mutant, the suicide plasmid pDM4-*pheS* (62) was used to construct pDM4-*pheS*-Δ*clpV4* (BTH_II1895). Briefly, the 819-bp upstream fragment and the 830-bp downstream fragment of *clpV4* were amplified with primer pairs D*clpV4*-F1/D*clpV4*-R1 and D*clpV4*-F2/D*clpV4*-R2, respectively. The upstream and downstream PCR fragments were fused together with the primer pair D*clpV4*-F1//D*clpV4*-R2 by overlap PCR (23). The resulting PCR products were digested with SpeI and BglII and inserted into similar digested pDM4-*pheS* to create pDM4-*pheS*-Δ*clpV4*. The knockout plasmids pDM4-*pheS*-Δ*icmF4* (BTH_II1885), pDM4-*pheS*-Δ*hcp4* (BTH_II1899), pDM4-*pheS*-Δ*clpV1* (BTH_I2958), pDM4-*pheS*-Δ*clpV2* (BTH_II0140), pDM4-*pheS*-Δ*clpV6* (BTH_II0264), pDM4-*pheS*-Δ*oxyR* (BTH_I1281), pDM4-*pheS*-Δ*katG* (BTH_I1282), pDM4-*pheS*-Δ*ahpC* (BTH_I2092), pDM4-*pheS*-Δ*mnoT* (BTH_I1598), pDM4-*pheS*-Δ*vgrG4a4b* (BTH_ II1893-1894), and pDM4-*pheS*-Δ*tseM* (BTH_II1883) were constructed in similar manners by using primers listed in Dataset S2.

To complement the *clpV4* mutant, primers *clpV4*-F/*clpV4*-R were used to amplify the *clpV4* gene fragment from *B. thailandensis* genomic DNA. The amplified DNA fragments were digested and then cloned into similar digested pME6032 plasmid, obtaining plasmid pME6032-*clpV4*. The complementary plasmids pME6032-*oxyR*, pME6032-*mnoT*, pME6032-*tseM*, pME6032-*vgrG4a*, pME6032-*vgrG4b*, pME6032-*icmF4*, pME6032-*clpV1*, pME6032-*clpV2*, pME6032-*clpV6*, pME6032-*aphC*, and pME6032-*katG* were constructed in similar manners as described above with primers listed in Dataset S2.

Site-directed mutagenesis was carried out by overlap PCR to substitute the histidine residue at position 63 of TseM into an alanine (TseM^{H63A}). The *tseM*^{H63A} DNA fragment was obtained by two rounds of PCR. Primer pairs *tseM*-F1/*tseMH63A*-R and *tseMH63A*-F/*tseM*-R1 were used to amplify segments 1 and 2, respectively. The second round of PCR was carried out by using *tseM*-F1/*tseM*-R1 as primer pair, whereas segment 1 and segment 2 together were used as templates to obtain the *tseM*^{H63A} fragment. The *tseM*^{H63A} DNA fragment was digested by BamHI/XhoI and cloned into similar digested pGEX6p-1 to produce pGEX6p-1-*tseM*^{H63A}. The primer pairs pGEX6p-1-F/*tseMN132R*-R and *tseMN132R*-F/pGEX6p-1-R were used to amplify the *tseM*$^{H63A/N132R}$ fragments by using the pGEX6p-1-*tseM*^{H63A} DNA as template in the first round PCR, and similarly cloned into pGEX6p-1 to produce pGEX6p-1-*tseM*$^{H63A/N132R}$ by using *tseM*-F1/*tseM*-R1 primers in the second round PCR. Next, the pGEX6p-1-*tseM*$^{H63A/N132R}$ DNA served as template to amplify the *tseM*$^{Q35R/H63A/N132R}$ fragments with primer pairs pGEX6p-1-F/*tseMQ35R*-R and *tseMQ35R*-F/pGEX6p-1-R, and *tseM*-F1/*tseM*-R1 or *tseZ*-F3/*tseZ*-R3 primer pairs were used in the second round PCR to produce the pGEX6p-1-*tseM*$^{Q35R/H63A/N132R}$ or pME6032-*tseM*$^{Q35R/H63A/N132R}$ plasmid, respectively. All constructs were validated by DNA sequencing.

In-Frame Deletion and Complementation in *B. thailandensis*. For constructing in-frame deletion mutants, the pDM4-*pheS* derivatives were transformed into relevant *B. thailandensis* strains through *E. coli* SM10(λpir)-mediated conjugational mating to carry out single crossover. The transconjugants were selected on LB agar medium containing chloramphenicol and streptomycin. Counter selection for markerless in-frame deletion was performed on M9 minimal medium agar plates with 0.4% glucose as a carbon source and 0.1% (wt/vol) *p*-chlorophenylalanine (62). For complementation, the pME6032 derivatives were transformed into relevant *B. thailandensis* strains by electroporation and the expression in *B. thailandensis* was induced by addition of 1 mM isopropyl β-D-1-thiogalactopyranoside (IPTG).

Overexpression and Purification of Recombinant Protein. To express and purify soluble GST- and His$_6$-tagged recombinant proteins, the pGEX6p-1, pET28a, and pET15b derivatives were transformed into *E. coli* XL1Blue, BL21(DE3), and *transB*(DE3) host strains, respectively. Bacteria were cultured at 37 °C in LB medium to an OD$_{600}$ of 0.5, shifted to 22 °C, induced with 0.5 mM IPTG, and then cultivated for an additional 12 h at 22 °C. Harvested cells were sonicated and proteins were purified with the His-Bind Ni-NTA resin or the GST-Bind resin (Novagen) according to manufacturer's instructions. Eluted recombinant proteins were dialyzed against PBS at 4 °C. Cleavage of the His$_6$ tag was performed by adding 10 units of Enterokinase-Max (Invitrogen) and incubation at 22 °C overnight. Ni-NTA agarose was used to remove the cleaved tag and uncleaved protein from the tag-free protein.

For purification of the insoluble recombinant MnoT, *E. coli* BL21 (DE3) containing pET15b-*mnoT* was grown in LB to an optical density at 600 nm of 0.6 after which 1 mM IPTG was added and growth was continued for 8 h at 26 °C. Recombinant MnoT accumulated in inclusion bodies were isolated as described (43). Briefly, the inclusion bodies were dissolved in 20 mM Tris·HCl, 100 mM glycine, 6 M urea (pH 8.3), and residual membranes were removed by centrifugation for 1 h at 200,000 × *g*. The protein was then refolded into its native conformation by diluting this stock solution 20-fold in refolding buffer containing 55 mM Tris·HCl, 0.21 mM sodium chloride, 0.88 mM potassium chloride, 880 mM L-arginine, and 0.5% 3-dimethyldodecylammoniopropane-sulfonate (SB-12) (Fluka), pH 7.0. After refolding overnight, the sample was dialyzed with 55 mM Tris·HCl (pH 6.5) containing 0.21 mM sodium chloride, 10 mM L-arginine, and 0.5% SB-12. The protein solution was filtered and stored at 4 °C. Proper folding was monitored by semi-native SDS/PAGE where the folded protein has a higher electrophoretic mobility than the denatured protein. The resulting proteins were stored at −80 °C until use. Protein concentrations were determined using the Bradford assay according to the manufacturer's instructions (Bio-Rad) with BSA as standard.

Fluorescence Dye-Based Intracellular ROS Detection. To detect intracellular ROS, the fluorescent reporter dye 2′,7′-dichlorodihydrofluorescein diacetate (H_2DCFDA) (Invitrogen) was used as previously described (32). Briefly, 1-mL samples were collected, washed with PBS, and then resuspended in 1 mL of PBS containing 10 μM H_2DCFDA. Samples were incubated in the dark for 20 min at 28 °C. The cells were then pelleted, the supernatant was removed, and they were resuspended in 1 mL M9 medium with 0.4% glucose containing 0.25 mM CHP. After a 30-min treatment

at 37 °C, the cells were pelleted, washed with PBS, resuspended in 1 mL of PBS, and then 200 μL of the resultant cell suspension was transferred to a dark 96-well plate. Fluorescence signals were measured using a SpectraMax M2 Plate Reader (Molecular Devices) with excitation/emission wavelengths of 495/520 nm. The results shown represented the mean of one representative assay performed in triplicate, and error bars represent SD. Statistical analysis was carried out with Student's *t* test.

Determination of Intracellular Ion Content. Intracellular ion content was determined as described previously (5, 13). Briefly, cells were grown in LB until stationary phase. After 20-mL culture solutions were collected and washed with PBS two times, the pellets were resuspended in 20 mL PBS buffer containing 0.4% glucose, 0.25 mM CHP, and 0.25 μM Mn^{2+}, and then incubated further for 20 min. These cultures were centrifuged at 1,575 × *g* for 10 min. The wet cell pellet weight was measured and bacteria were chemically lysed using Bugbuster (Novagen) according to the manufacturer's instructions. Bacteria were resuspended in Bugbuster solution by pipetting and incubation on a rotating mixer at a slow setting for 10 h. Total protein for each sample was measured by using NanoDrop ND-1000 spectrophotometer (NanoDrop Technologies) according to the manufacturer's instructions. Each sample was diluted 100-fold in 2% molecular grade nitric acid to a total volume of 5 mL. Samples were analyzed by inductively coupled plasma mass spectrometry (ICP-MS) (Varian 802-MS), and the results were corrected using the appropriate buffers for reference and dilution factors. Triplicate cultures of each strain were analyzed during a single experiment and the experiment was repeated at least three times.

Sensitivity Assays. Stationary phase *B. thailandensis* strains grown in LB medium were collected, washed, and diluted 30-fold into M9 medium containing 25 nM Mn^{2+} (or as indicated), and treated with CHP (0.25 mM), H_2O_2 (1.0 mM), $CdCl_2$ (0.1 mM), or diamide (0.35 mM), respectively, at 37 °C for 40 min. After treatment, the cultures were serially diluted and plated onto LB agar plates, and colonies were counted after 36-h growth at 37 °C. Percentage survival was calculated by dividing number of cfu of stressed cells by number of cfu of cells without stress (32). All these assays were performed in triplicate at least three times.

Quantitative Real-Time PCR. Bacteria were harvested during the mid-exponential phase and RNA was extracted using the RNAprep Pure Cell/Bacteria Kit and treated with RNase-free DNase (Tiangen). The purity and concentration of the RNA were determined by gel electrophoresis and spectrophotometer (NanoDrop, Thermo Scientific). First-strand cDNA was reverse transcribed from 1 μg of total RNA with the TransScript First-Strand cDNA Synthesis SuperMix (TransGen Biotech). Quantitative real-time PCR (qRT-PCR) was performed in CFX96 Real-Time PCR Detection System (Bio-Rad) with TransStart Green qPCR SuperMix (TransGen Biotech). For all primer sets (Dataset S2), the following cycling parameters were used: 95 °C for 30 s followed by 40 cycles of 94 °C for 15 s and 50 °C for 30 s. For standardization of results, the relative abundance of 16S rRNA was used as the internal standard.

Western Blot Analysis. Western blot analysis was performed as previously described (23). Samples were resolved by SDS/PAGE and transferred onto PVDF membranes (Millipore). The membrane was blocked in 5% (wt/vol) nonfat milk powder for 4 h at room temperature and incubated with primary antibodies at 4 °C overnight: anti-TseM (BTH_II1883) rabbit polyclonal antibody, 1:1,000; anti-ICDH, 1:6,000; anti-His (Millipore), 1:1,000; and anti-GST (Zhongshan Gold Bridge), 1:1,000. The membrane was washed three times in TBST buffer (50 mM Tris, 150 mM NaCl, 0.05% Tween 20, pH 7.4) and incubated with 1:5,000 dilution of horseradish peroxidase-conjugated secondary antibodies (Shanghai Genomics) for 1 h. Signals were detected using the ECL Plus Kit (GE Healthcare) following the manufacturer's specified protocol. The ICDH antisera were made in our previous studies (64). The purified His-tagged TseM and Hcp4 were used to generate rabbit anti-TseM and anti-Hcp4 polyclonal antibodies and the resulting antiserum was affinity purified against the same proteins.

EMSA. Electrophoretic mobility shift assay was performed using biotin 5′-end-labeled promoter probes. Bio-P_{T6SS-4} was amplified from *B. thailandensis* genomic DNA with primers T6p-oxyR-F-5′ biotin/T6p-oxyR-R-5′ biotin. The unlabeled P_{T6SS-4} competitor DNA was amplified from *B. thailandensis* genomic DNA with primers T6p-oxyR-F/T6p-oxyR-R. All PCR fragments were purified by EasyPure Quick Gel Extraction Kit (TransGen Biotech). Each 20-μL EMSA reaction solution was prepared by adding the following components according to the manufacturer's protocol (LightShift Chemiluminescent EMSA Kit; Thermo Fisher Scientific): 1× binding buffer, 50 ng poly (dI-dC), 2.5% glycerol, 0.05% Nonidet P-40, 5 mM $MgCl_2$, 3 ng biotin-DNA, 1 ng unlabeled DNA as competitor, and different concentrations of proteins. Reaction solutions were incubated for 20 min at room temperature. The protein-probes mixture was separated in a 6% polyacrylamide native gel and transferred to a Biodyne B nylon membrane (Thermo Fisher Scientific). Migration of biotin-labeled probes was detected by streptavidin-horseradish peroxidase conjugates that bind to biotin and chemiluminescent substrate according to the manufacturer's protocol.

***G. mellonella* Infection Model.** The *G. mellonella* larvae infection model was used to evaluate the virulence of *B. thailandensis* mutants as described (45, 46). *G. mellonella* were purchased from Livefood JiaYing Ltd (TianJin) and maintained in the dark at 25 °C until use. Bacteria grown to OD_{600} of 1.6 in LB at 37 °C were harvested, washed, and resuspended in phosphate-buffered saline (PBS) to give a final concentration of 10^5 bacteria. Twenty *G. mellonella* larvae were injected with a 50-μL dose of 10^5 cfu in the secondary right proleg using a Hamilton H syringe and then incubated statically at 37 °C for 16 h before determining survival rates. A total of 50 μL PBS was injected as control to measure any potential lethal effects of the injection process, or larvae were not injected to measure the effects of the incubation procedure. Each experiment was performed in triplicate.

Metal-Free apo-TseM Preparation and Metal Ion Binding Assays. Metal-free apo-TseM was prepared as described previously (65). Briefly, proteins were dialyzed overnight at 4 °C against 250 μM EDTA and 5 mM *o*-phenanthroline in 50 mM Hepes (pH 8.0), 150 mM NaCl, and 10% (vol/vol) glycerol, followed by three dialysis steps in 50 mM Hepes (pH 8.0), 150 mM NaCl, and 10% (vol/vol) glycerol to remove EDTA and *o*-phenanthroline.

Mn^{2+} binding was measured using isothermal titration calorimetry (ITC) at 25 °C with a NANO-ITC 2G microcalorimeter (TA Instruments) (66). The 1 mM $MnSO_4$ solution used for titration was prepared with the apo-TseM dialysis buffer. The protein concentration in the sample solution was 50 μM. All protein and metal solutions were extensively degassed before titration. After a stable baseline had been achieved, the $MnSO_4$ titration was performed with a total of 25 injections of 5 μL into the protein solutions (volume = 1.5 mL) until the protein sample was saturated with Mn^{2+}. A control experiment in the absence of protein was performed to measure the heat generated due to Mn^{2+} dilution in the buffer. Blank titrations of the $MnSO_4$ solution into the dialysis buffer were performed to correct for the dilution heat of the zinc solution. Data reduction and analyses were performed with the Nano Analyze software (TA Instruments), and an independent binding model was used. All ITC experiments were performed in triplicate.

Mn^{2+} binding was also detected using the metal reconstitution assay as previously described (67). Briefly, for removing as much of the ions as possible, purified TseM protein (100 μM) was added to the solution containing 25 mM Tris, 25 mM diethylene triamine pentaacetic acid, and 10% glycerol at pH 7.5 and put on ice. After 1 h, the protein solution was dialyzed with buffer (25 mM Tris, 10% glycerol, pH 7.5) at 4 °C. For reconstitution with metal ions, the resulting TseM protein (10 μM) was added to 25 μM of the desired divalent-metal ions (Fe^{3+}, Mn^{2+}, Mg^{2+}, Cd^{2+}, and Zn^{2+}) and put on ice for 30 min, with Milli-Q water for preparing ions solution as the control. These solutions were dialyzed again (25 mM Tris, 10% glycerol, pH 7.5) as mentioned above to remove unbound metal ions and the metal ions bound to the protein were analyzed using atomic absorption spectroscopy (ZEEnit 650P; Analytik Jena).

Zn^{2+} binding of proteins was detected using the Zn^{2+}-binding dye 4-(2-pyridylazo)-resorcinol (PAR) as previously reported (68). An iron-binding assay was performed with ferrous sulfate as previously described (69).

Intrabacterial and Interbacterial Growth Competition Assays. Intrabacterial competition assays were conducted as described previously with minor modifications (70). In brief, overnight-grown competitor and participant strains were washed with M9 medium before mixing for competition. The initial competitor–participant ratio was 1:1 (OD_{600} of 2.0 for each strain) and the bacteria were incubated for 12 h at 37 °C in liquid M9 medium containing 20 μM CHP and 25 nM Mn^{2+}. The competitor strains contained pME6032, conferring tetracycline resistance for selection. After competition, the competitor and participant colonies were counted on LB plates supplemented with tetracycline and streptomycin or streptomycin alone, and changes in the competitor/participant ratios were determined. Data from all competitions were analyzed using the Student's *t* test.

Interbacterial competition assays were conducted as described (22, 71) with minor modifications. Briefly, overnight cultures of relevant *B. thailandensis* (streptomycin resistance) and the *E. coli* K12 competitors containing pME6032 vector or pME6032-*mnoT* (tetracycline resistance) were washed three times with M9 medium, adjusted to OD_{600} of 1.6, and then mixed in 10:1 (vol/vol) of relevant *B. thailandensis* versus the competitor *E. coli* K12. To calculate the initial cfu ratio of relevant *B. thailandensis* and competitor, 100 μL of the mixture was taken out, serially diluted, spread on LB plates containing different antibiotic, and incubated at 37 °C for 36 h. For competition assays, CHP (final concentration 50 μM) was added to the above residual mixture (2 mL) and incubated at 37 °C 100 rpm. After 12 h, the mixture was serially diluted, spread on LB plates containing different antibiotics, and the final cfu ratio was determined.

GST Pull-Down Assay. The GST pull-down assay was performed as previously described with minor modifications (64, 72). Briefly, 0.5 mg purified GST fusion protein was mixed with cleared cell lysates collected from CHP-treated *B. thailandensis* culture (200 mL) on a rotator for 3 h at 4 °C, and 100 μL prewashed glutathione beads were added to the reactions. After another 2 h of incubation at 4 °C, the beads were washed five times with PBS. Proteins associated with beads were treated with SDS sample buffer, resolved by SDS/PAGE, and visualized by silver staining (Bio-Rad). Individual protein gel bands were excised, digested with trypsin, and analyzed by matrix-assisted laser desorption/ionization/mass spectrometry (Voyager-DESTR, Applied Biosystems). To analyze protein interactions with purified proteins, purified GST-TseM was mixed with His_6-MnoT in PBS on a rotator for 2 h at 4 °C, and GST was used as a negative control. After adding 40 μL of a prewashed glutathione beads slurry, binding was allowed to proceed for another 2 h at 4 °C. The beads were then washed five times with TEN buffer [100 mM Tris-Cl (pH 8.0), 10 mM EDTA, 500 mM NaCl]. Retained proteins were detected by immunoblot after SDS/PAGE using the anti-His antibody (Millipore).

Amino Acid Sequence Alignment and 3D Modeling Prediction. Sequence alignment and database searches were carried out using BLAST programs at the BLAST server of the National Center for Biotechnology Information (NCBI) website (https://www.ncbi.nlm.nih.gov/) and visualized by using BioEdit (www.mbio.ncsu.edu/bioedit/bioedit.html). The construction of phylogenetic tree was made with MEGA 6.0 program. The 3D models of TseM were generated using Phyre^2 (www.sbg.bio.ic.ac.uk/~phyre2/html/page.cgi?id=index).

RNA-Seq Experiment. Total RNA was extracted from *B. thailandensis* wild type and the Δ*oxyR* mutant (three biological replicates) grown in LB at 37 °C with shaking (220 rpm) to a final optical density of ~1.6, using bacteria total RNA isolation kit (Tiangen). RNA degradation and contamination was monitored on 1% agarose gels; RNA purity was checked using the NanoPhotometer spectrophotometer (Implen) and RNA integrity was assessed using the Bioanalyzer 2100 system (Agilent Technologies). A total of 3 μg RNA per sample was used as input material in RNA sample preparations for subsequent cDNA library construction. All six samples had RIN values above 7.0. Sequencing libraries were generated using Illumina HiSeq 2000 RNA Sample Preparation Kit (Illumina) following manufacturer's recommendations and four index codes were added to attribute sequences to each sample. Differential expression analysis was performed using the NOIseq method (Sonia Tarazona 2100). *P* values were adjusted using the Benjamini–Hochberg method. Corrected *P* value of 0.05 and $\log_2$ (fold change) of 0.8 were set as the threshold for significantly differential expression. Gene Ontology (GO) enrichment analysis of differentially expressed genes was implemented by the GOseq R package, in which gene length bias was corrected. GO terms with corrected *P* values of less than 0.05 were considered significantly enriched by differential expressed genes.

Statistical Analysis. Statistical analyses of survival assay, intracellular ion content determination, ROS determination, and expression data were performed using paired two-tailed Student's *t* test. Statistical analyses were performed using GraphPad Prism Software (GraphPad Software).

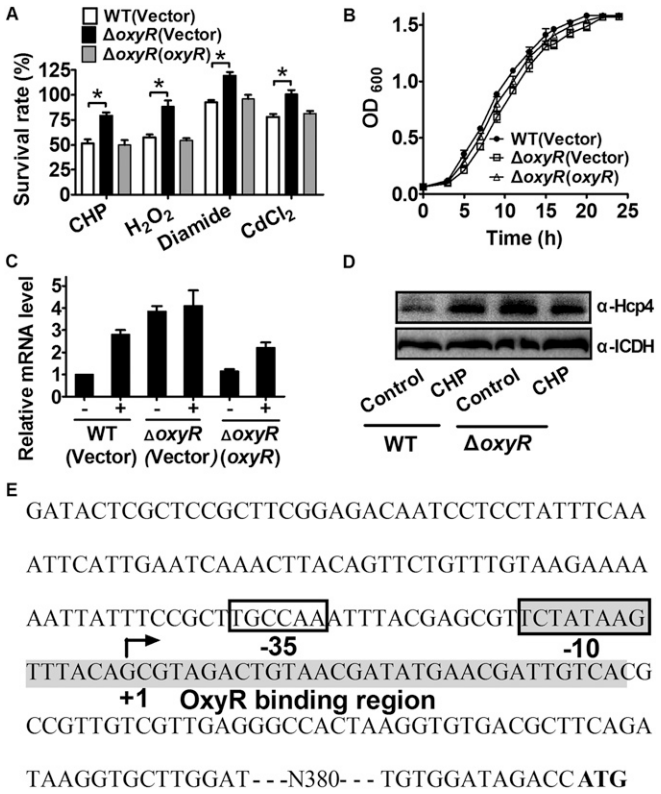

Fig. S1. OxyR regulates the expression of T6SS-4. (*A*) The Δ*oxyR* mutant was highly resistant to oxidative stress. The survival rate was measured by viability assay. Mean values with SDs (error bars) from at least three repeats are shown. **P* < 0.05. (*B*) Growth curves of the wild-type (WT), Δ*oxyR* mutant, and the complemented strain Δ*oxyR*(*oxyR*) under normal condition. The growth of the indicated strains in LB was monitored by measuring OD_{600} at indicated time points. (*C*) The levels of *hcp4* mRNAs in exponentially growing *B. thailandensis* cells with (+) or without (–) 20-min exposure to 0.15 mM CHP was determined by quantitative RT-PCR. The mRNA levels are presented relative to the value obtained from WT cells without CHP treatment. (*D*) The protein level of Hcp4 in differently treated WT and Δ*oxyR* mutant strains. Lysates from bacteria with or without (control) 30-min exposure to 0.15 mM CHP were resolved by SDS/PAGE, and Hcp4 was detected by immunoblotting using a specific anti-Hcp4 antibody. For the pellet fraction, isocitrate dehydrogenase (ICDH) was used as a loading control. (*E*) Identification of the OxyR binding site in the promoter region of T6SS-4. Putative OxyR binding site identified by the online software Virtual Footprint (www.prodoric.de/vfp) was indicated by shading. The ATG start codon of the first ORF of the T6SS-4 operon was marked in boldface, and the –35 and –10 elements of the T6SS-4 promoter are boxed. +1 denotes the transcription start point.

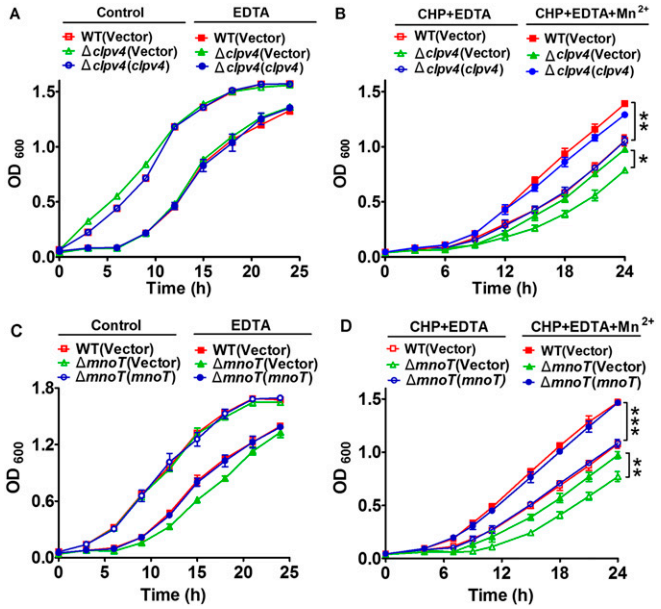

Fig. S2. T6SS-4 and MnoT are required for optimal growth under oxidative stress. Saturated bacterial cultures were diluted to an OD_{600} of 0.05 in LB medium (*A* and *C*); LB medium with 250 μM EDTA (*A* and *C*); LB medium with 240 μM CHP and 250 μM EDTA (*B* and *D*); and LB medium with 240 μM CHP, 250 μM EDTA, and 250 μM Mn^{2+} (*B* and *D*). The growth of the cultures was monitored by measuring OD_{600} at indicated time points. Data shown were the average of three independent experiments; error bars indicate SD from three independent experiments. ***$P < 0.001$; **$P < 0.01$; *$P < 0.05$.

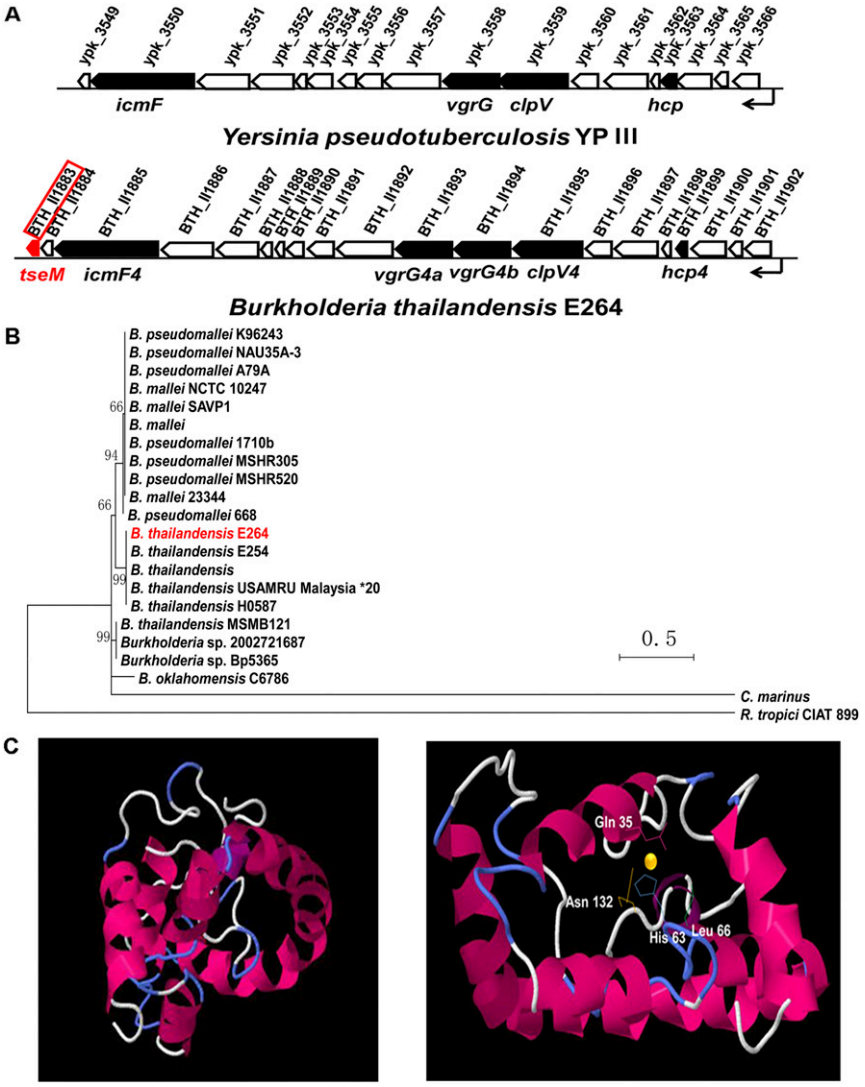

Fig. S3. Identification of a putative T6SS effector in the *B. thailandensis* T6SS-4 gene cluster. (*A*) The structure of *B. thailandensis* T6SS-4 gene cluster is similar to the T6SS-4 gene cluster from *Y. pseudotuberculosis*. The *tseM* gene (*bth_II1883*, indicated in red) localizes in the end of the T6SS-4 operon. (*B*) Phylogenetic relationship of *B. thailandensis* TseM with homologous proteins in other relative *Burkholderia*. Different protein sequences were obtained from the SwissProt database. The phylogenetic tree was constructed using MEGA 6.0 by the neighbor-joining method and multiple sequence alignment was performed using CLUSTAL W. The scale bar indicates percentage of divergence (distance). Accession numbers are as follows: *B. thailandensis* E264 (ABC35934); *B. thailandensis* E254 (AIT22423); *B. thailandensis* (AIP65980); *B. thailandensis* USAMRU Malaysia (AIC89753); *B. thailandensis* MSMB121 (AGK49752); *B. mallei* (AIO54172); *B. mallei* SAVP1 (ABM48775); *B. mallei NCTC* 10247 (AIS27138); *B. pseudomallei* 668 (ABN88025); *B. pseudomallei* A79A (AIV92858); *B. pseudomallei* K96243 (YP_110555); *B. pseudomallei* NAU35A-3 (AIS91265); *B. oklahomensis* C6786 (AJX34588); *Burkholderia* sp. 2002721687 (AJY39125); *Burkholderia* sp. Bp5365 (ALX46218); *Celeribacter marinus* IMCC12053_1024 (ALI54972.1); and *Rhizobium tropici* CIAT 899 (AGB70070.1). (*C*) Side and top 3D model of TseM-ion binding built with phyre[2]. The ion is illustrated as a yellow sphere.

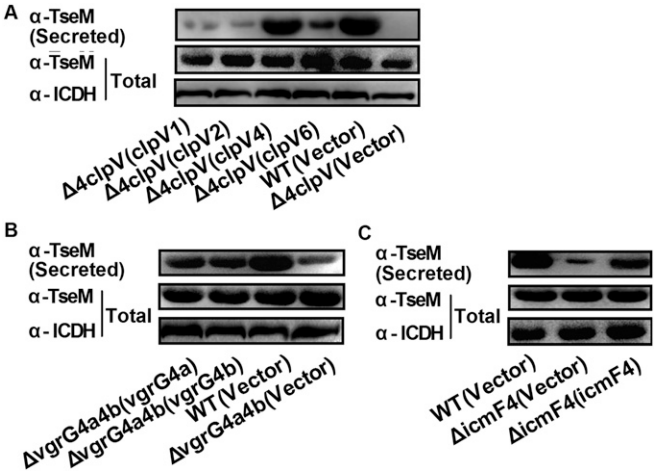

Fig. S4. Effects of different *clpV*s and *vgrGs* on TseM secretion. (*A*) Secretion of TseM in the Δ4*clpV* mutant complemented with *clpV1*, *clpV2*, *clpV4*, and *clpV6*, respectively. (*B*) Secretion of TseM in the Δ*vgrG4a4b* mutant complemented with *vgrG4a* and *vgrG4b*, respectively. (*C*) Secretion of TseM in the Δ*icmF4* mutant and the complemented strain. Proteins in culture supernatant were probed using specific anti-TseM antibody. For the pellet fraction, isocitrate dehydrogenase (ICDH) was used as a loading control.

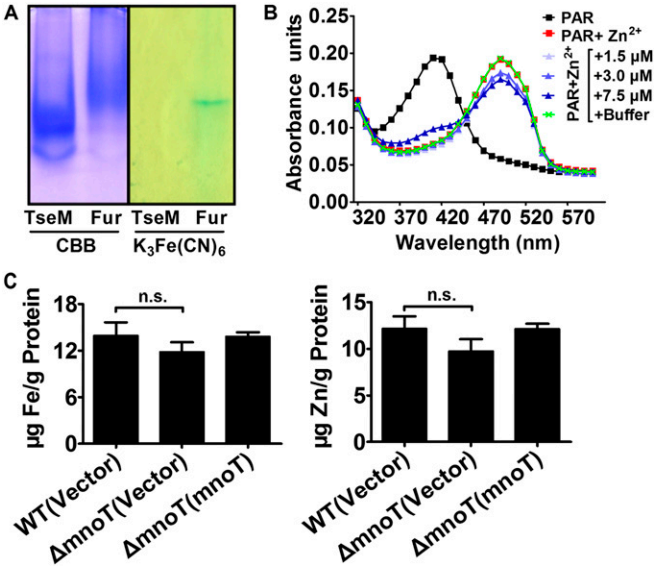

Fig. S5. TseM and MnoT are not involved in iron and zinc accumulation. (*A*) TseM (BTH_II1883) does not bind iron. Iron binding analysis by 15% native PAGE. Lanes 1 and 2 show the gel stained with Coomassie bright blue. Lanes 3 and 4 show the same gel stained for iron by the potassium ferricynaide method. His_6-Fur was used as a positive control. Lanes 1 and 3 show TseM (BTH_II1883). Lanes 2 and 4 show His_6-Fur. (*B*) TseM (BTH_II1883) does not bind Zn^{2+}. Spectral scans of solutions containing 10 μM PAR without Zn^{2+} (black), with Zn^{2+} (red), or with Zn^{2+} and increasing concentrations of recombinant TseM (BTH_II1883) and control buffer (different color) are shown. (*C*) MnoT is not involved in iron and zinc accumulation in *B. thailandensis*. Stationary phase *B. thailandensis* strains were exposed to 0.25 mM CHP for 20 min in PBS containing 1 μM $FeCl_3$ or 1 μM $ZnSO_4$. Iron and zinc ions associated with bacterial cells were measured using ICP-MS. Data shown are the average and SD from three independent experiments. n.s., not significant.

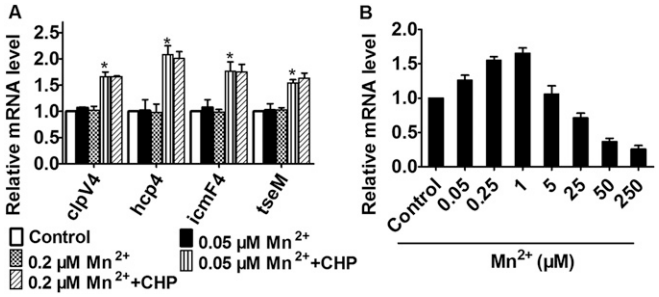

Fig. S6. Effects of Mn^{2+} and CHP on T6SS-4 and *mnoT* expression. (*A*) *B. thailandensis* wild type was grown in M9 medium containing different concentrations of Mn^{2+} with or without CHP (100 μM), and the expression of *clpV4*, *hcp4*, *icmF4*, and *tseM* was measured by qRT-PCR. (*B*) The expression of *mnoT* is regulated by Mn^{2+}. *B. thailandensis* wild type was grown in M9 medium containing different concentrations of Mn^{2+}, and the expression of *mnoT* was measured by qRT-PCR. Data shown were the average of three independent experiments; error bars indicate SD from three independent experiments. $^*P < 0.05$.

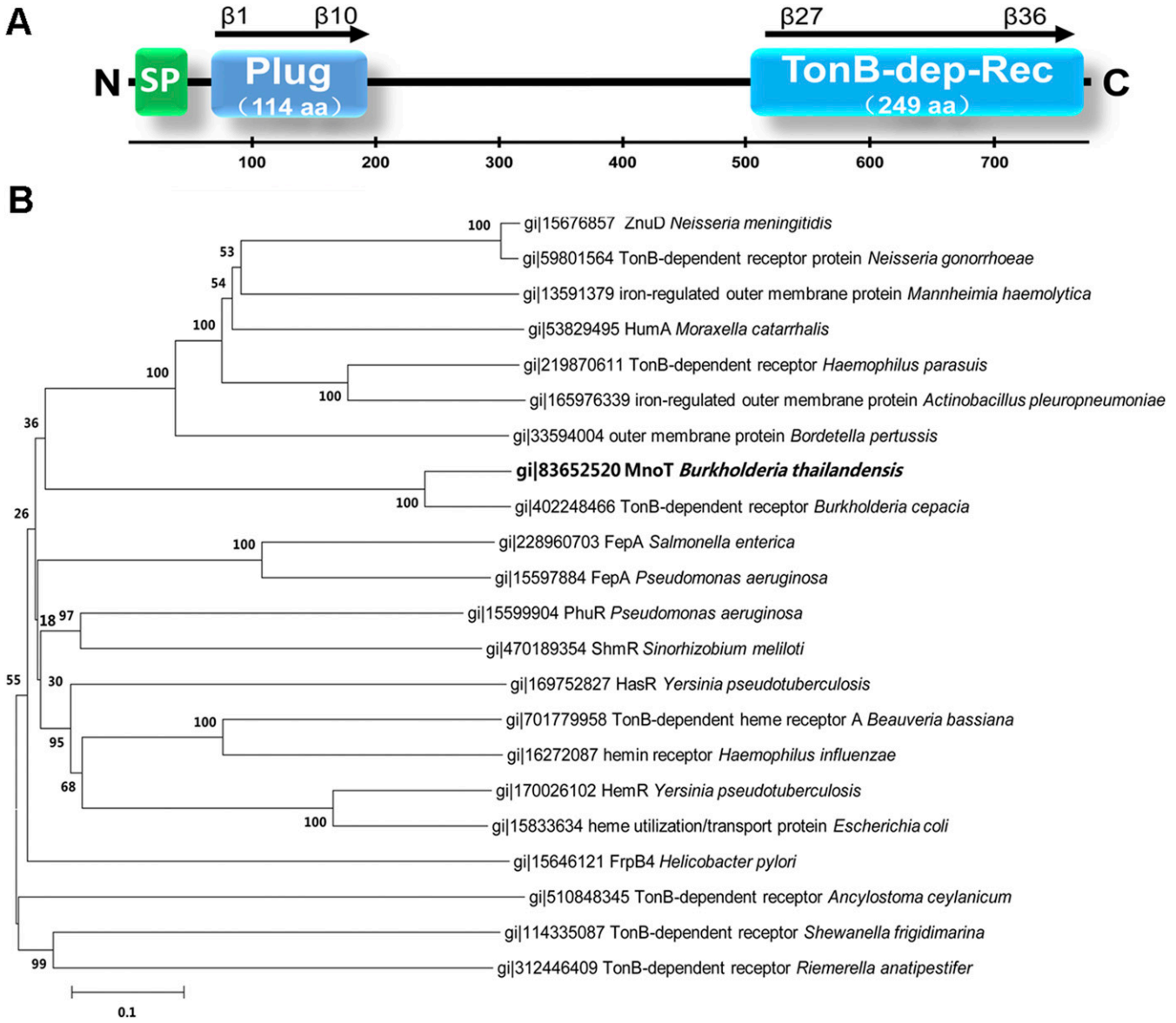

Fig. S7. Sequence analysis of MnoT. (*A*) Pertinent secondary structure elements of MnoT. Plug, the TonB-plug domain (residues 68–181); TonB-dep-Rec, the TonB-dependent receptor domain (residues 529–777). (*B*) Phylogenetic relationship of TonB-dependent outer membrane receptors. Different protein sequences were obtained from the SwissProt database. The phylogenetic tree was constructed using MEGA 6.0 by the neighbor-joining method and multiple sequence alignment was performed using CLUSTAL W. The scale bar indicates percentage of divergence (distance). SwissProt accession nos. of proteins from species are as follows: *B. thailandensis* BTH_I1598 (gi:83652520); *N. meningitidis* ZnuD (gi:15676857); *Neisseria gonorrheae* TonB-dependent receptor protein (gi:59801564); *Mannheimia haemolytica* iron-regulated outer membrane protein (gi:13591379); *Moraxella catarrhalis* HumA (gi:53829495); *Haemophilus parasuis* TonB-dependent receptor (gi:219870611); *Actinobacillus pleuropneumoniae* iron-regulated outer membrane protein (gi:165976339); *Bordetella pertussis* outer membrane protein (gi:33594004); *Burkholderia cepacia* TonB-dependent receptor (gi:402248466); *Salmonella enterica* FepA (gi:228960703); *Pseudomonas aeruginosa* FepA (gi:15597884); *Pseudomonas aeruginosa* PhuR (gi:15599904); *Sinorhizobium meliloti* ShmR (gi:470189354); *Y. pseudotuberculosis* HasR (gi:169752827); *Beauveria bassiana* TonB-dependent heme receptor A (gi:701779958); *Haemophilus influenzae* hemin receptor (gi:16272087); *Y. pseudotuberculosis* HemR (gi:170026102); *E. coli* heme utilization/transport protein (gi:15833634); *Helicobacter pylori* FrpB4 (gi:15646121); *Ancylostoma ceylanicum* TonB-dependent receptor (gi:510848345); *Shewanella frigidimarina* TonB-dependent receptor (gi:114335087); and *Riemerella anatipestifer* TonB-dependent receptor (gi:312446409).

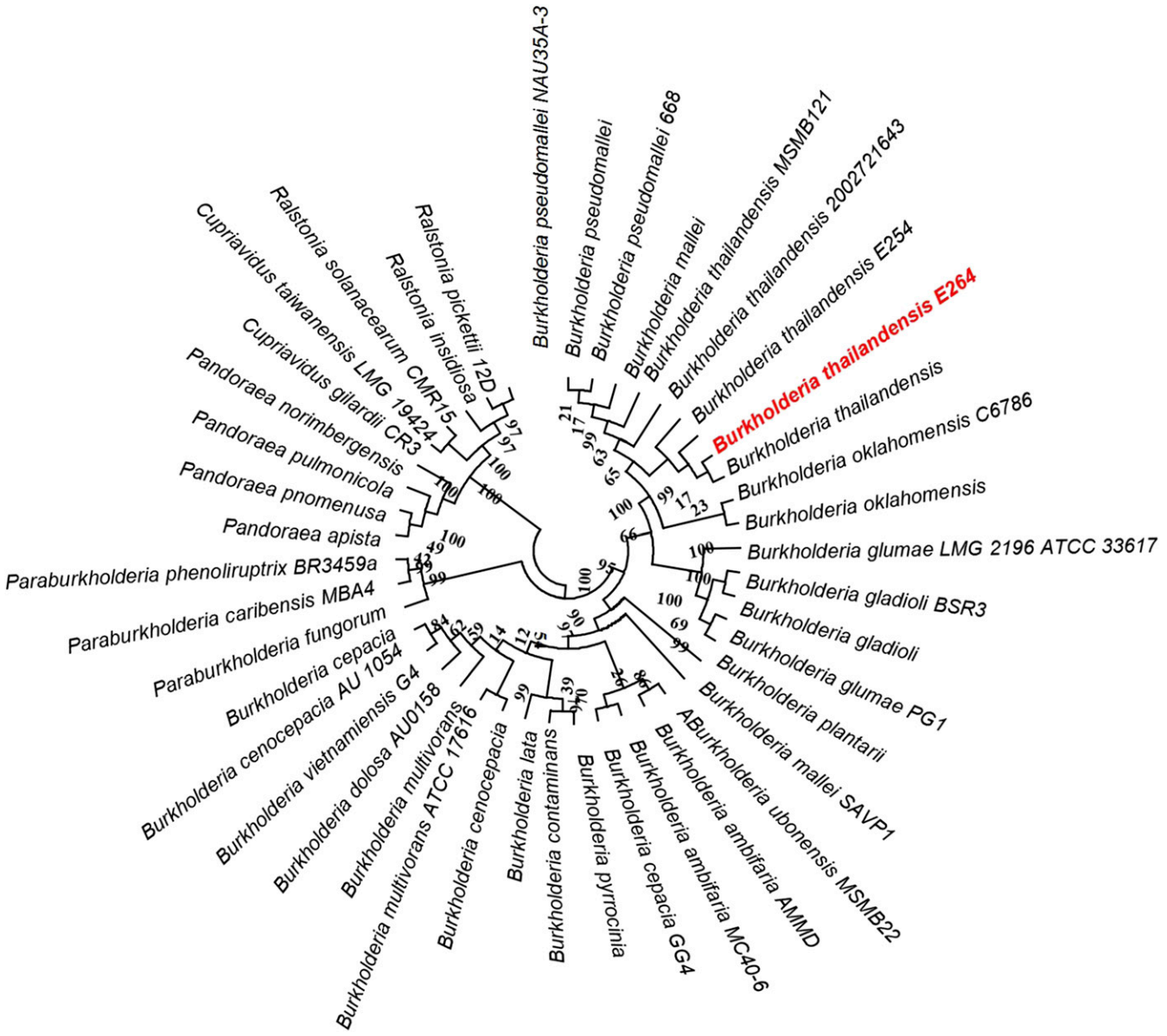

Fig. S8. MnoT homologs are widely distributed in *Burkholderia* species. The phylogenetic tree generated by the minimum-evolution algorithm in MEGA 6.0 illustrates that MnoT is highly conserved among the vast majority of *Burkholderia*. The *B. thailandensis* E264 MnoT was indicated in red. The bar represents the genetic distance.

Dataset S1. Differentially transcribed genes in Δ*oxyR* mutant compared with the *B. thailandensis* E264 wild-type detected by RNA-seq

Dataset S1

Dataset S2. Bacterial strains, plasmids, and primers used in this study

Dataset S2

Dataset S1. Differentially transcribed genes in Δ*oxyR* mutant compared to the *B. thailandensis* E264 wild-type detected by RNA-seq.

CDS	Gene	Predicted function	[a]Fold change
BTH_II0169	*fliM*	flagellar motor switch protein	4.2
BTH_II0216		major facilitator transporter	3.5
BTH_II0217		hippurate hydolase	2.8
BTH_II0271		transposase	2.1
BTH_II0285		hypothetical protein	1.9
BTH_II0287		enoyl-CoA hydratase	3.7
BTH_II0336		opine dehydrogenase	1.8
BTH_II0341		50S ribosomal protein L15	11.7
BTH_II0347		hypothetical protein	3.5
BTH_II0407		glutathione S-transferase	3.4
BTH_II0471		NADH oxidase	1.9
BTH_II0472		benzoate 1,2-dioxygenase subunit beta	2.5
BTH_II0473		benzoate 1,2-dioxygenase subunit alpha	2.7
BTH_II0481		cytochrome C oxidase subunit III	4.7
BTH_II0482		cytochrome C oxidase subunit III	5.6
BTH_II0483		muconolactone delta-isomerase	4.8
BTH_II0484		catechol 1,2-dioxygenase	5.3
BTH_II0485		muconate cycloisomerase	4.6
BTH_II0487		AraC family transcriptional regulator	1.9
BTH_II0488	*ohbB*	ortho-halobenzoate 1,2-dioxygenase alpha-ISP protein	5.2
BTH_II0489		anthranilate 1,2-dioxygenase	5.7
BTH_II0490		Rieske (2Fe-2S) protein	5.7
BTH_II0491		FAD-dependent pyridine nucleotide-disulfide oxidoreductase	5.8
BTH_II0492		HIT family hydrolase	2.6
BTH_II0493		phospholipase	1.9
BTH_II0504	*cheW*	chemotaxis protein	2.1
BTH_II0544		UDP-glucose 6-dehydrogenase	1.9
BTH_II0577		threonine transporter RhtB	1.8
BTH_II0578		hypothetical protein	2.0
BTH_II0628		allantoin permease family protein	3.3
BTH_II0642		spermidine/putrescine ABC transporter ATP-binding protein	2.6
BTH_II0694		polysaccharide biosynthesis protein	2.2
BTH_II0695		glycosyl transferase family 1	1.7
BTH_II0741		hypothetical protein	2.0
BTH_II0743		type III secretion system protein	2.2
BTH_II0744		ATP synthase	2.8
BTH_II0745	*sctL*	type III secretion system protein	2.1
BTH_II0746		hypothetical protein	3.9
BTH_II0747		lipoprotein transmembrane protein	2.9
BTH_II0748		HPr kinase	2.9
BTH_II0749		hypothetical protein	2.8
BTH_II0751	*sctV*	type III secretion inner membrane protein	1.9
BTH_II0753		Surface presentation of antigens	1.8
BTH_II0754	*sctR*	type III secretion inner membrane protein	1.8

BTH_II0755	*scts*	type III secretion inner membrane protein	2.6
BTH_II0757		hypothetical protein	2.3
BTH_II0758		serine protease	2.0
BTH_II0759		hypothetical protein	3.2
BTH_II0775		pilM family protein	1.8
BTH_II0791		cellulose synthase	2.0
BTH_II0792		glycosyl hydrolases 8 family protein	3.1
BTH_II0793		cellulose biosynthesis protein	1.8
BTH_II0794		hypothetical protein	1.9
BTH_II0822	*orgA*	oxygen-regulated invasion protein	2.3
BTH_II0825	*yscF*	type III secretion protein	2.0
BTH_II0826	*bsaM*	type III secretion protein	2.9
BTH_II0837	*bsaX*	type III secretion system protein	2.6
BTH_II0838	*bsay*	type III secretion system protein	2.0
BTH_II0840	*bicA*	type III secretion chaperone	2.4
BTH_II0841	*bipB*	translocator protein BipB	2.6
BTH_II0843	*bprA*	DNA-binding protein	2.1
BTH_II0844	*bprD*	translocator protein	2.1
BTH_II0849	*icsB*	virulence protein	2.5
BTH_II0850	*bicP*	type III secretion chaperone	2.5
BTH_II0853		AraC family transcriptional regulator	3.2
BTH_II0863		type VI secretion protein Rhs	1.9
BTH_II0877		N-acetylmuramoyl-L-alanine amidase	2.8
BTH_II0895		hypothetical protein	1.6
BTH_II0964		hypothetical protein	2.4
BTH_II0975		aldolase	2.6
BTH_II0976		HPr kinase	3.4
BTH_II0977		3-hydroxyisobutyrate dehydrogenase	3.3
BTH_II0985		C4-dicarboxylate ABC transporter substrate-binding protein	2.8
BTH_II0992	*secD*	preprotein translocase subunit	2.0
BTH_II1028		methyltransferase	1.7
BTH_II1096		GntR family transcriptional regulator	1.8
BTH_II1097		sugar MFS transporter	4.0
BTH_II1110		SIS domain protein	3.6
BTH_II1111		isoaspartyl peptidase	2.1
BTH_II1133		membrane protein	1.8
BTH_II1168	*cobA*	uroporphyrin-III C-methyltransferase	2.4
BTH_II1202		sel1 repeat family protein	2.5
BTH_II1203		TonB-denpendent receptor	2.0
BTH_II1332		caudovirales tail fiber assembly family protein	1.9
BTH_II1346		tail protein	2.0
BTH_II1348		phage head protein	2.6
BTH_II1362		phage transcriptional activator, Ogr/Delta	2.0
BTH_II1386		putative transmembrane regulator	2.9
BTH_II1409	*hisM*	histidine/lysine/arginine/ornithine ABC transporter permease	2.0
BTH_II1410	*hisQ*	histidine/lysine/arginine/ornithine ABC transporter permease	1.8
BTH_II1418		magnesium ABC transporter ATPase	3.0
BTH_II1419		metA-pathway of phenol degradation family protein	2.3
BTH_II1501		3-phenylpropionate dioxygenase	2.0

BTH_II1502		hypothetical protein	2.2
BTH_II1503		Rieske (2Fe-2S) protein	2.2
BTH_II1593		aromatic amino acid aminotransferase	2.3
BTH_II1594		aromatic amino acid transporter	3.0
BTH_II1596		hypothetical protein	1.7
BTH_II1660		hypothetical protein	2.0
BTH_II1726		**ABC transporter permease**	4.2
BTH_II1785		transposase, Mutator family protein	2.2
BTH_II1837		leucine/isoleucine/valine transporter permease subunit	2.2
BTH_II1838	*livH*	branched-chain amino acid transporter permease subunit	2.8
BTH_II1869		AraC family transcriptional regulator	2.4
BTH_II1883	***tseM***	**hypothetical protein**	1.8
BTH_II1885	*imcF4*	type VI secretion system protein	1.9
BTH_II1886		OmpA domain protein	2.2
BTH_II1887	*impJ4*	type VI secretion protein	1.9
BTH_II1888		hypothetical protein	2.2
BTH_II1889		type VI secretion protein	2.9
BTH_II1890		type VI secretion protein	3.1
BTH_II1891		pentapeptide repeat-containing protein	3.6
BTH_II1892		type VI secretion protein	2.9
BTH_II1893	***vgrG4a***	**type IV secretion protein**	2.8
BTH_II1894	***vgrG4b***	**type IV secretion protein**	3.8
BTH_II1895	***clpV4***	**type IV secretion ATP-dependent protease**	4.2
BTH_II1896	*impH4*	type VI secretion protein	3.8
BTH_II1897	*impG4*	type VI secretion protein	3.8
BTH_II1898	*impF4*	type VI secretion protein	3.9
BTH_II1899	***hcp4***	**type VI secretion protein**	4.5
BTH_II1900	*impC4*	hypothetical protein	3.5
BTH_II1901		type VI secretion protein	2.1
BTH_II1902	*impA4*	type VI secretion protein	2.1
BTH_II1943		XRE family transcriptional regulator	2.1
BTH_II2051	*phnV*	2-aminoethylphosphonate ABC transport system, membrane component	5.5
BTH_II2052		2-aminoethylphosphonate ABC transporter, permease protein	2.0
BTH_II2131		ABC transporter substrate-binding protein	2.7
BTH_II2139		TonB-dependent heme/hemoglobin receptor family protein	1.8
BTH_II2141		**hemin ABC transporter substrate-binding protein**	4.3
BTH_II2218		peptide ABC transporter permease	3.3
BTH_II2219		peptide ABC transporter substrate-binding protein	2.6
BTH_II2235		citrate lyase subunit beta	2.3
BTH_II2251		Uncharacterized small protein	3.6
BTH_II2252		carbon starvation protein A	3.3
BTH_II2261		membrane protein	2.8
BTH_II2265		peptidase A24A	2.7
BTH_II2269		ghypothetical protein	3.2
BTH_II2303		2-oxoisovalerate dehydrogenase subunit beta	1.7
BTH_II2304		2-oxoisovalerate dehydrogenase subunit alpha	1.9
BTH_II2325		hypothetical protein	3.0
BTH_I0024	*lrgA*	murein hydrolase transporter	2.7
BTH_I0082		hypothetical protein	2.8

BTH_I0205		transporter	1.7
BTH_I0292		short-chain dehydrogenase	1.9
BTH_I0371		sel1 repeat family protein	1.8
BTH_I0452		membrane protein	15.6
BTH_I0467		hypothetical protein	14.1
BTH_I0640		major facilitator transporter	1.7
BTH_I0704		LysR family transcriptional regulator	1.9
BTH_I0746		chromate transporter	1.9
BTH_I1020		potassium-transporting ATPase	2.7
BTH_I1125	*lpxC*	UDP-3-O-(3-hydroxymyristoyl) glucosamine N-acyltransferase	3.3
BTH_I1173		peptidase S10	2.0
BTH_I1174		hypothetical protein	1.8
BTH_I1203		C4-dicarboxylate transport protein	2.7
BTH_I1204		allantoicase	2.5
BTH_I1218		4-hydroxy-2-oxoglutarate aldolase/2-deydro-3-deoxyphosphogluconate aldolase	2.1
BTH_I1282	***katG***	**catalase/peroxidase HPI**	4.7
BTH_I1283		hypothetical protein	7.0
BTH_I1284	*dpsA*	starvation-inducible DNA-binding protein	2.0
BTH_I1351	*rfbP*	undecaprenyl-phosphate galactosephosphotransferase	3.4
BTH_I1359		glycosyl transferase	3.3
BTH_I1414		membrane transport solute-binding protein	1.8
BTH_I1447		TnpC protein	7.5
BTH_I1449		TnpC protein	12.5
BTH_I1556		maltose ABC transporter, ATP-binding protein	2.3
BTH_I1598	***mnoT***	**TonB-dependent outer member receptor**	**1.7**
BTH_I1690		membrane protein	9.9
BTH_I1820	*hutH*	histidine ammonia-lyase	3.1
BTH_I1821		histidine utilization repressor	3.4
BTH_I1822	*hutU*	urocanate hydratase	1.8
BTH_I1872		hypothetical protein	2.8
BTH_I1919		hypothetical protein	3.9
BTH_I1953		peptide synthetase-domain protein	2.4
BTH_I2089	*ispD*	2-C-methyl-D-erythritol 4-phosphate cytidylyltransferase	2.4
BTH_I2090	*ispF*	2-C-methyl-D-erythritol 2,4-cyclodiphosphate synthase	2.9
BTH_I2091	***ahpD***	**alkyl hydroperoxidase**	15.8
BTH_I2092	***ahpC***	**alkyl hydroperoxidase**	10.7
BTH_I2176		Ser/Thr phosphatase	1.9
BTH_I2294		conserved hypothetical protein	2.0
BTH_I2405		magnesium chelatase	1.9
BTH_I2429		hypothetical protein	1.9
BTH_I2461		probable CpaA2 pilus assembly protein	7.0
BTH_I2496		hypothetical protein	1.9
BTH_I2545		peptidase	1.8
BTH_I2570		ISBm1, transposase orfA, interruption-N	1.8
BTH_I2644		sugar ABC transporter, periplasmic sugar-binding protein	2.1
BTH_I2645		sugar ABC transporter, permease protein	2.1
BTH_I3167		flagellar biosynthesis protein FlhG	2.8
BTH_I3183		chemotaxis protein CheY	2.2

BTH_I3189		H-NS histone family protein	1.8
BTH_I3196		flagellin	2.0
BTH_I3197		flagellar hook protein FliD	2.1
BTH_I3198		conserved hypothetical protein	2.0
BTH_I3203		hypothetical protein	2.0
BTH_I3330		branched-chain amino acid ABC transporter, ATP-binding protein	2.9
BTH_I3331		amino acid ABC transporter ATP-binding protein	2.9
BTH_II0001		hypothetical protein	-1.9
BTH_II0004		DNA-binding protein	-1.7
BTH_II0005	*kbl*	2-amino-3-ketobutyrate CoA ligase	-4.8
BTH_II0006	*tdh*	L-threonine 3-dehydrogenase	-5.5
BTH_II0012		succinylglutamate desuccinylase / aspartoacylase family protein	-3.3
BTH_II0033		amino acid transporter	-1.9
BTH_II0055		FAD-dependent pyridine nucleotide-disulfide oxidoreductase	-2.6
BTH_II0056		probable porin or abc transporter protein	-2.2
BTH_II0057		hypothetical protein	-3.0
BTH_II0058	*acrB*	multidrug transporter AcrB	-2.6
BTH_II0067		cybP	-3.6
BTH_II0103	*opcP*	outer membrane porin	-1.8
BTH_II0105		hypothetical protein	-2.0
BTH_II0106		ribbon-helix-helix	-2.0
BTH_II0163	*flhA*	flagellar biosynthesis protein	-1.7
BTH_II0210		ribose ABC transporter permease	-1.7
BTH_II0251	*vasD*	type VI secretion system protein	-1.8
BTH_II0254	*impL*	type VI secretion system protein	-2.2
BTH_II0255	*impM*	type VI secretion system protein	-4.6
BTH_II0256		serine/threonine protein kinase	-2.5
BTH_II0257	*impA*	type VI secretion system protein	-3.6
BTH_II0258		hypothetical protein	-3.3
BTH_II0259	*impC*	type VI secretion system protein	-2.4
BTH_II0260		hypothetical protein	-2.5
BTH_II0262	*impG*	type VI secretion system protein	-3.1
BTH_II0274		alpha/beta hydrolase family protein	-2.8
BTH_II0275		comA operon protein	-2.1
BTH_II0276		fatty acyl-AMP ligase	-2.5
BTH_II0277		amidohydrolase family superfamily	-6.5
BTH_II0278	*jamB*	stearoyl-CoA desaturase (Delta-9 desaturase)	-6.7
BTH_II0279		**cyclopropane-fatty-acyl-phospholipid synthase**	-6.2
BTH_II0280		polyketide synthase	-7.1
BTH_II0281	*jamB*	stearoyl-CoA desaturase (Delta-9 desaturase)	-8.9
BTH_II0322		hypothetical protein	-2.1
BTH_II0327		benzoate 1,2-dioxygenase	-2.1
BTH_II0343		polymer-forming cytoskeletal family protein	-2.3
BTH_II0360		carboxymuconolactone decarboxylase	-1.8
BTH_II0361		gcupin	-1.9
BTH_II0362		succinate dehydrogenase iron-sulfur subunit	-2.4
BTH_II0363		hypothetical protein	-3.0
BTH_II0365		RC180	-2.0
BTH_II0368		hypothetical protein	-2.3

BTH_II0372		beta-lactamase	-2.6
BTH_II0396		membrane protein	-5.4
BTH_II0414		OsmY domain-containing protein	-2.3
BTH_II0415		phosphofructokinase	-2.6
BTH_II0416	*ackA*	acetate kinase	-3.3
BTH_II0417		phosphate acetyltransferase	-4.3
BTH_II0418		poly-beta-hydroxybutyrate polymerase	-3.0
BTH_II0419	*atpD*	F0F1 ATP synthase subunit beta	-2.6
BTH_II0420		F0F1 ATP synthase subunit epsilon	-3.8
BTH_II0421		**ATP synthase I**	-3.9
BTH_II0422		lipoprotein	-5.2
BTH_II0423	*atpB*	F0F1 ATP synthase subunit A	-5.0
BTH_II0424		ATP synthase F0	-5.1
BTH_II0425		ATP synthase F0 subunit B	-2.5
BTH_II0426	*atpA*	F0F1 ATP synthase subunit alpha	-3.5
BTH_II0427	*atpG*	ATP synthase F1 subunit gamma	-2.8
BTH_II0428		alcohol dehydrogenase	-3.8
BTH_II0429		hypothetical protein	-3.5
BTH_II0437		ABC-2 type transport system permease protein	-2.8
BTH_II0438		ABC transporter	-5.9
BTH_II0439		glycoside hydrolase family 43	-5.3
BTH_II0440		RND efflux system, outer membrane protein	-2.6
BTH_II0441		TetR family transcriptional regulator	-2.4
BTH_II0442		universal stress protein UspA	-4.5
BTH_II0443		hypothetical protein	-3.8
BTH_II0444		ABC transporter permease	-5.1
BTH_II0445		putative ABC transport system ATP-binding protein	-4.8
BTH_II0446		HlyD family secretion protein	-5.1
BTH_II0447		RND transporter	-3.6
BTH_II0450		adenylylsulfate kinase	-2.0
BTH_II0451		hypothetical protein	-2.3
BTH_II0454		putative lysine decarboxylase family protein	-3.3
BTH_II0538		rubrerythrin	-4.3
BTH_II0539		hypothetical protein	-3.5
BTH_II0596		hypothetical protein	-1.8
BTH_II0762	*hrpB*	AraC family transcriptional regulator	-4.2
BTH_II0786		hypothetical protein	-1.7
BTH_II0787		ATP-dependent protease	-2.6
BTH_II0788		hypothetical protein	-1.9
BTH_II0821		hypothetical protein	-2.2
BTH_II0855	*impL*	type VI secretion system protein	-2.4
BTH_II0857	*impJ*	type VI secretion protein	-2.1
BTH_II0867		hypothetical protein	-2.0
BTH_II0888		hypothetical protein	-1.9
BTH_II0889		AraC family transcriptional regulator	-2.1
BTH_II0900		nitrate reductase/sulfite reductase flavoprotein alpha-component	-1.6
BTH_II0902		peptidase propeptide and YPEB domain protein	-2.0
BTH_II0911		hypothetical protein	-1.9
BTH_II0912		hypothetical protein	-3.9

BTH_II0916	*groL*	molecular chaperone	-3.1
BTH_II0917		hypothetical protein	-3.9
BTH_II0918		ribose-phosphate pyrophosphokinase	-4.7
BTH_II0919		**NAD synthetase**	-3.1
BTH_II0920		histidine kinase	-3.0
BTH_II0921		hypothetical protein	-3.4
BTH_II0922	*ald*	alanine dehydrogenase	-4.1
BTH_II0923		hypothetical protein	-4.7
BTH_II0924		molecular chaperone Hsp20	-4.4
BTH_II0925		beta-lactamase	-2.2
BTH_II0926		hypothetical protein	-2.5
BTH_II0927		acetyl-CoA synthetase	-3.4
BTH_II0928		pyruvate dehydrogenase (acetyl-transferring) E1 component, alpha	-5.9
BTH_II0929		pyruvate dehydrogenase subunit beta	-5.5
BTH_II0930		branched-chain alpha-keto acid dehydrogenase subunit E2	-3.6
BTH_II0938	*glgX*	glycogen operon protein	-3.6
BTH_II0939	*glgB*	glycogen branching protein	-4.3
BTH_II0940		glycogen synthase	-3.1
BTH_II0941		alpha-glucan phosphorylase	-3.7
BTH_II0942		hypothetical protein	-2.2
BTH_II0943		fatty acyl-AMP ligase	-2.9
BTH_II0944		cytochrome C	-2.7
BTH_II0956		hypothetical protein	-2.0
BTH_II0966		glycine/betaine ABC transporter ATP-binding protein	-2.3
BTH_II0968		AraC family transcriptional regulator	-4.3
BTH_II0991		AraC family transcriptional regulator	-1.8
BTH_II1000		diguanylate cyclase	-2.4
BTH_II1001		30S ribosomal protein S21	-2.4
BTH_II1002		cold-shock protein	-2.0
BTH_II1008	*cheY*	chemotaxis protein	-1.8
BTH_II1009		sensor kinase	-2.2
BTH_II1010		MFS transporter	-2.1
BTH_II1020		gp56-like protein	-4.0
BTH_II1043		terminase	-2.0
BTH_II1054		tail assembly protein	-3.1
BTH_II1060		hydrolase Nlp/P60	-1.9
BTH_II1061		phage tail assembly protein	-2.7
BTH_II1073	***betB***	**betaine-aldehyde dehydrogenase**	-2.0
BTH_II1082		transposase, Mutator family protein	-1.9
BTH_II1084		cytochrome B561	-2.3
BTH_II1087		membrane protein	-2.0
BTH_II1180		electron transfer DM13 family protein	-2.7
BTH_II1185		metal transporter	-1.8
BTH_II1191		hypothetical protein	-3.1
BTH_II1195		short-chain dehydrogenase	-1.7
BTH_II1196		arabinose ABC transporter substrate-binding protein	-2.1
BTH_II1244		Crp/Fnr family transcriptional regulator	-3.9
BTH_II1245	*cheY*	chemotaxis protein	-4.3
BTH_II1257		spermidine synthase	-2.1

BTH_II1258		phosphate ABC transporter permease	-1.7
BTH_II1259		hypothetical protein	-1.9
BTH_II1267		hypothetical protein	-2.6
BTH_II1274		polyketide cyclase	-2.1
BTH_II1291		hemolysin D	-2.1
BTH_II1293		multidrug ABC transporter ATP-binding protein	-3.2
BTH_II1294		ABC transporter permease	-3.0
BTH_II1297		hypothetical protein	-1.7
BTH_II1298	*ftsH*	cell division protein	-2.7
BTH_II1299		peptidase	-2.0
BTH_II1309		ATPase	-3.0
BTH_II1311		Mg^{2+}-importing ATPase	-4.6
BTH_II1312		hypothetical protein	-2.0
BTH_II1314		Uncharacterized conserved protein	-2.5
BTH_II1315		hypothetical protein	-3.3
BTH_II1316		hypothetical protein	-3.3
BTH_II1349		phage small terminase subunit	-2.6
BTH_II1423		Uncharacterised protein family (UPF0187) superfamily	-2.3
BTH_II1428		2OG-Fe(II) oxygenase superfamily protein	-2.8
BTH_II1429		peptidase S8	-4.3
BTH_II1440		RpiR family transcriptional regulator	-8.1
BTH_II1441		D-alanyl-D-alanine dipeptidase	-10.8
BTH_II1442		**ABC transporter substrate-binding protein**	-9.6
BTH_II1443		peptide ABC transporter permease	-7.2
BTH_II1444		cytochrome C550	-4.9
BTH_II1445		peptide ABC transporter ATP-binding protein	-5.6
BTH_II1446		ABC transporter	-6.0
BTH_II1447		LysR family transcriptional regulator	-2.4
BTH_II1532		porin	-1.9
BTH_II1566		universal stress protein A	-2.4
BTH_II1567		universal stress protein A	-2.6
BTH_II1568		universal stress protein A	-3.6
BTH_II1574		hypothetical protein DP43_5211	-2.5
BTH_II1577		hypothetical protein	-1.8
BTH_II1653		hypothetical protein	-2.1
BTH_II1654		peptidase M23 family protein	-2.4
BTH_II1655		ABC transporter substrate-binding protein	-2.3
BTH_II1657		methylmalonate-semialdehyde dehydrogenase	-2.7
BTH_II1658		beta alanine--pyruvate aminotransferase	-2.6
BTH_II1668		polyketide biosynthesis enoyl-CoA hydratase	-2.7
BTH_II1671		polyketide beta-ketoacyl:ACP synthase	-2.4
BTH_II1672		acyl carrier protein	-2.2
BTH_II1680		hypothetical protein	-2.2
BTH_II1681		LuxR family transcriptional regulator	-2.5
BTH_II1697	*gcN5*	N-acetyltransferase GCN5	-2.0
BTH_II1698		enoyl-ACP reductase	-2.3
BTH_II1794		TetR family transcriptional regulator	-2.4
BTH_II1795		long-chain fatty acid--CoA ligase	-3.7
BTH_II1796		long-chain fatty acid--CoA ligase	-2.9

BTH_II1802		AMP-dependent synthetase	-3.3
BTH_II1806		membrane protein	-2.3
BTH_II1808		oxidoreductase	-2.4
BTH_II1832	*pchB*	isochorismate-pyruvate lyase	-1.7
BTH_II1856		LysR family transcriptional regulator	-3.1
BTH_II1862		drug:proton antiporter	-1.9
BTH_II1865		N-methylproline demethylase	-1.9
BTH_II1866		4-vinyl reductase	-2.3
BTH_II1868	*glyA*	serine hydroxymethyltransferase	-1.9
BTH_II1915		MFS transporter	-4.2
BTH_II1928		membrane protein	-2.0
BTH_II1957	*copC*	copper resistance protein	-2.3
BTH_II1960		RND transporter	-2.4
BTH_II1963		phosphoesterase	-2.0
BTH_II1975		glycosyl transferase	-1.8
BTH_II2030		hypothetical protein	-3.2
BTH_II2062		hypothetical protein	-2.4
BTH_II2078		Uncharacterized ACR, YkgG family COG1556 family	-1.8
BTH_II2079		iron-sulfur cluster binding protein	-2.2
BTH_II2083		acyl-CoA dehydrogenase	-2.2
BTH_II2105		transporter	-2.1
BTH_II2106		hemolysin secretion protein	-4.3
BTH_II2107	*lipH*	alpha/beta hydrolase	-3.6
BTH_II2113		hypothetical protein	-2.9
BTH_II2124		O-methyltransferase	-2.7
BTH_II2125		aerotaxis receptor	-1.8
BTH_II2144		membrane protein	-4.0
BTH_II2145		penicillin-binding protein	-3.8
BTH_II2148		membrane protein	-2.0
BTH_II2149		ubiquinol oxidase subunit II, cyanide insensitive	-2.1
BTH_II2151		hypothetical protein	-2.1
BTH_II2154		sugar MFS transporter	-2.0
BTH_II2169		hypothetical protein	-1.9
BTH_II2181		radical SAM domain protein	-2.1
BTH_II2182		hypothetical protein	-2.1
BTH_II2192		hypothetical protein	-3.8
BTH_II2211		transporter	-3.1
BTH_II2258		sugar translocase	-2.3
BTH_II2264		hypothetical protein	-10.9
BTH_II2268		bacterial type II and III secretion system family protein	-2.0
BTH_II2272	*tadG*	pilus assembly protein	-3.0
BTH_II2282		membrane protein	-1.8
BTH_II2292		hypothetical protein	-3.4
BTH_II2296		4'-phosphopantetheinyl transferase	-1.9
BTH_II2300		transcriptional regulator	-2.2
BTH_II2310		FAD-dependent pyridine nucleotide-disulfide oxidoreductase	-1.9
BTH_II2314		aminoglycoside phosphotransferase	-2.2
BTH_II2315		nitroreductase family protein	-1.9
BTH_II2316		transporter	-4.2

BTH_II2317		CBS domain protein	-2.9
BTH_II2318		nitroreductase	-3.5
BTH_II2319		hypothetical protein	-4.2
BTH_II2320		hypothetical protein	-3.3
BTH_II2322		polysaccharide deacetylase family protein	-2.0
BTH_II2323		GTP-binding protein	-3.1
BTH_II2333		hydrophobe/amphiphile efflux family protein	-2.4
BTH_II2340		4'-phosphopantetheinyl transferase	-2.0
BTH_II2344		ABC transporter permease	-2.3
BTH_II2351		ABC transporter	-2.2
BTH_II2371	*parA*	chromosome partitioning protein	-2.0
BTH_II2372	*parB*	chromosome partitioning protein	-2.4
BTH_I0020		hypothetical protein	-3.9
BTH_I0031	*fliQ*	flagellar biosynthesis protein	-3.0
BTH_I0034		SAM-dependent methyltransferase	-1.9
BTH_I0046		branched-chain amino acid ABC transporter ATP-binding protein	-2.1
BTH_I0079		lipoprotein	-2.3
BTH_I0081	*speG*	GCN5 family N-acetyltransferase	-2.5
BTH_I0088	*rpoD*	RNA polymerase sigma factor	-2.7
BTH_I0089		hypothetical protein	-2.8
BTH_I0090		LTXXQ motif family protein	-2.7
BTH_I0094		preprotein translocase	-2.6
BTH_I0144	*mreD*	rod shape-determining protein	-2.2
BTH_I0159		HAD family hydrolase	-1.8
BTH_I0164	*hslU*	ATP-dependent protease	-2.9
BTH_I0165	***hslV***	**peptidase**	-2.3
BTH_I0168	*cobW*	cobalamin biosynthesis protein	-2.1
BTH_I0180		multidrug DMT transporter permease	-3.0
BTH_I0185		5-dehydro-4-deoxyglucarate dehydratase	-2.2
BTH_I0191		NAD-dependent dehydratase	-2.0
BTH_I0192		coniferyl aldehyde dehydrogenase	-4.6
BTH_I0193		acyl-CoA dehydrogenase	-2.1
BTH_I0194		GMC family oxidoreductase	-3.1
BTH_I0195	*fliK*	flagellar hook-length control protein	-2.8
BTH_I0198	*fliH*	flagellar assembly protein	-5.7
BTH_I0268		hypothetical protein	-3.2
BTH_I0283		copper-translocating P-type ATPase	-4.3
BTH_I0284		LemA family protein	-2.0
BTH_I0285		membrane protein	-2.7
BTH_I0286		membrane protein	-4.0
BTH_I0298		sugar kinase	-2.2
BTH_I0299		N-acylglucosamine 2-epimerase	-3.0
BTH_I0300		LacI family transcription regulator	-2.1
BTH_I0302		membrane protein	-1.7
BTH_I0304		hypothetical protein	-2.0
BTH_I0305		porin	-1.9
BTH_I0308		alpha/beta hydrolase	-2.4
BTH_I0309		AsnC family transcriptional regulator	-2.0
BTH_I0340	*bioA*	adenosylmethionine--8-amino-7-oxononanoate aminotransferase	-1.7

BTH_I0521		glycosyl transferase	-1.9
BTH_I0537		glycosyl transferase family 1	-2.8
BTH_I0541		DSBA oxidoreductase	-1.8
BTH_I0544		amino acid deaminase	-2.0
BTH_I0545		transcriptional regulator	-3.5
BTH_I0546		D-aminoacylase	-3.5
BTH_I0558		regulatory protein	-1.9
BTH_I0563		TetR family transcriptional regulator	-2.7
BTH_I0564		acyl-CoA dehydrogenase	-3.6
BTH_I0565		3-hydroxyacyl-CoA dehydrogenase	-4.1
BTH_I0572		metal ABC transporter permease	-1.8
BTH_I0584	*glyS*	glycyl-tRNA synthetase subunit beta	-1.8
BTH_I0590	*phoH*	phosphate starvation protein	-2.0
BTH_I0600		glycerol-3-phosphate dehydrogenase	-1.9
BTH_I0617		membrane protein	-1.9
BTH_I0618		chemotaxis protein	-2.5
BTH_I0621		nitrate ABC transporter ATP-binding protein	-2.4
BTH_I0622		sulfonate ABC transporter permease	-2.2
BTH_I0624		DeoR family transcriptional regulator	-2.7
BTH_I0625		nicotinate phosphoribosyltransferase	-4.2
BTH_I0626		phosphoribosyl transferase	-2.9
BTH_I0675		serine protease	-2.5
BTH_I0676		carboxypeptidase regulatory-like domain protein	-2.9
BTH_I0698		HAD family hydrolase	-2.0
BTH_I0699		sugar ABC transporter ATP-binding protein	-2.1
BTH_I0715		hypothetical protein BTRA_3301	-2.2
BTH_I0716		cyclopropane-fatty-acyl-phospholipid synthase	-2.2
BTH_I0719		thioredoxin	-2.2
BTH_I0792		CDP-6-deoxy-delta-3,4-glucoseen reductase	-1.7
BTH_I0850		hypothetical protein	-2.0
BTH_I0880		drug resistance MFS transporter, drug:H+ antiporter-2 family protein	-1.9
BTH_I0944		membrane protein	-2.7
BTH_I0945		nitrate reductas	-4.7
BTH_I0946		acetylpolyamine aminohydrolase	-3.1
BTH_I0952		multidrug DMT transporter permease	-2.5
BTH_I0953		glyoxalase	-3.7
BTH_I0954		aminotransferase class I and II family protein	-3.0
BTH_I0955		heat shock protein 90	-2.4
BTH_I0956		chorismate--pyruvate lyase	-1.9
BTH_I1001		major facilitator superfamily MFS_1 domain protein	-2.2
BTH_I1002		lipocalin-like domain protein	-2.0
BTH_I1003		cold-shock protein	-1.9
BTH_I1005		phospholipase	-2.8
BTH_I1006		hypothetical protein	-4.2
BTH_I1007	*xanP*	xanthine permease	-3.9
BTH_I1034		glycosyl transferase	-2.9
BTH_I1092		hypothetical protein	-1.8
BTH_I1163	*accB*	acetyl-CoA carboxylase	-2.3
BTH_I1165		thioredoxin family protein	-1.8

BTH_I1175		transcriptional regulator	-3.1
BTH_I1176		2-dehydro-3-deoxygalactonokinase	-2.9
BTH_I1177		4-hydroxy-2-oxoglutarate aldolase/2-dehydro-3-deoxyphosphogluconat	-2.1
BTH_I1197		major facilitator family transporter	-2.3
BTH_I1263		hypothetical protein	-2.5
BTH_I1264		hypothetical protein	-11.1
BTH_I1266		membrane protein	-1.7
BTH_I1306	*grpE*	co-chaperone GrpE	-2.5
BTH_I1307		conserved hypothetical protein	-2.2
BTH_I1308	*dnaK*	molecular chaperone DnaK	-4.0
BTH_I1364		flagellar transcriptional activator FlhD	-1.9
BTH_I1387		Bacterial protein of unknown function (DUF883) superfamily	-1.9
BTH_I1409		xanthine dehydrogenase, C-terminal subunit	-2.2
BTH_I1425		glycerophosphoryl diester phosphodiesterase	-1.7
BTH_I1457	*groES-1*	chaperonin	-2.1
BTH_I1458	*groL-1*	chaperone GroEL	-1.8
BTH_I1465	*pyrB-1*	aspartate carbamoyl transferase	-1.8
BTH_I1484		undecaprenyl-phosphate alpha-N-acetylglucosaminyl transferase	-2.0
BTH_I1503		branched-chain amino acid ABC transporter	-2.2
BTH_I1562		outer membrane lipoprotein carrier protein LolA	-2.0
BTH_I1611		xanthine/uracil permease family protein	-3.5
BTH_I1612		adenosine deaminase	-2.8
BTH_I1649		hydrolase, alpha/beta fold family	-2.5
BTH_I1653		electron transfer flavoprotein subunit beta	-2.2
BTH_I1655		acyl-CoA dehydrogenase	-3.1
BTH_I1687		conserved hypothetical protein	-2.1
BTH_I1702		acetyltransferase	-2.1
BTH_I1703		membrane protein	-2.0
BTH_I1704		molybdopterin biosynthesis moeA protein	-1.9
BTH_I1750		Protein of unknown function (DUF461) family	-2.0
BTH_I1751		SCO1/SenC family protein	-2.2
BTH_I1788		ubiquinol oxidase subunit II	-4.2
BTH_I1791		hypothetical protein	-3.0
BTH_I1793		NifU-like domain protein	-2.4
BTH_I1800	*hemN-2*	oxygen-independent coproporphyrinogen III oxidase	-2.6
BTH_I1801		cyclic nucleotide-binding domain protein	-2.6
BTH_I1802		membrane protein	-3.0
BTH_I1804		peptidase	-2.3
BTH_I1811		lipoprotein	-1.9
BTH_I1845		**nitrogen regulation protein**	-2.2
BTH_I1852		nitrate reductase	-2.6
BTH_I1855		nitrate/nitrite transporter NarK	-2.4
BTH_I1918		pyocin R2_PP, tail formation	-4.2
BTH_I1933		hypothetical protein	-11.6
BTH_I1939		peptidyl-prolyl cis-trans isomerase	-1.8
BTH_I1982		NLP/P60 family protein	-3.6
BTH_I1994	*aceB*	malate synthase A	-2.4
BTH_I1995	*dehII-1*	haloacid dehalogenase	-2.7
BTH_I1996		LysR family transcriptional regulator	-2.8

BTH_I1997		universal stress protein family	-1.8
BTH_I1999		ATP-dependent RNA helicase RhlE	-2.4
BTH_I2000		acyl-CoA-binding protein	-2.1
BTH_I2058		GMP synthase	-2.1
BTH_I2063		muramoyltetrapeptide carboxypeptidase	-2.1
BTH_I2068		conserved hypothetical protein	-2.6
BTH_I2069		allantoicase	-3.4
BTH_I2070		ureidoglycolate hydrolase	-3.6
BTH_I2071		Protein of unknown function (DUF989) superfamily	-2.5
BTH_I2081		PspA/IM30 family protein	-2.0
BTH_I2171		2-hydroxy-3-oxopropionate reductase	-3.2
BTH_I2173	*gcl*	glyoxylate carboligase	-4.8
BTH_I2178		conserved hypothetical protein	-1.8
BTH_I2205		ATP-dependent Clp protease, ATP-binding subunit ClpB	-2.9
BTH_I2215		multidrug resistance protein	-1.7
BTH_I2216		MerR family transcriptional regulator	-2.0
BTH_I2273		outer membrane protein, OmpW family	-3.3
BTH_I2292		membrane protein	-2.2
BTH_I2297		major facilitator family transporter	-1.8
BTH_I2298	*tkrA*	2-ketogluconate reductase	-2.0
BTH_I2316		mechanosensitive ion channel protein	-1.8
BTH_I2318		cytochrome c family protein	-2.6
BTH_I2326		ApbE family protein	-2.8
BTH_I2327		ABC transporter ATP-binding protein	-3.6
BTH_I2328		transporter	-2.2
BTH_I2344		sugar ABC transporter permease	-1.7
BTH_I2357		thioesterase type II	-2.4
BTH_I2358		lipase/esterase	-3.0
BTH_I2359		pyridine nucleotide-disulphide oxidoreductase	-4.1
BTH_I2360		nonribosomal peptide synthetas	-5.2
BTH_I2361		phosphotransferase	-5.4
BTH_I2362		acyl-CoA dehydrogenase	-6.7
BTH_I2363		polyketide synthase	-6.1
BTH_I2364		peptide synthetase	-4.8
BTH_I2365		polyketide synthase	-5.4
BTH_I2366		polyketide synthase	-5.6
BTH_I2367		dihydroaeruginoic acid synthetase	-4.9
BTH_I2368		hypothetical protein	-3.9
BTH_I2369		AraC family transcriptional regulator	-3.6
BTH_I2370		outer membrane porin OpcP	-2.5
BTH_I2375		hypothetical protein	-4.7
BTH_I2383		arginine/ornithine antiporter	-2.8
BTH_I2384	*arcA*	arginine deiminase	-4.7
BTH_I2385	*arcC*	carbamate kinase	-3.9
BTH_I2386	*arcC*	carbamate kinase	-3.6
BTH_I2387		short-chain dehydrogenase	-1.7
BTH_I2391		MarR family transcriptional regulator	-2.3
BTH_I2392		major facilitator family transporter	-4.2
BTH_I2393		fenI protein	-3.0

BTH_I2402		glycosyl hydrolase	-2.0
BTH_I2413		conserved hypothetical protein	-2.1
BTH_I2414		conserved hypothetical protein	-1.8
BTH_I2418		peptide synthetase-like protein	-1.7
BTH_I2423		iron ABC transporter	-2.3
BTH_I2435		ribose ABC transporter, periplasmic ribose-binding protein	-3.3
BTH_I2447		Peptidase family M23/M37	-2.7
BTH_I2448		amino acid ABC transporter, permease protein	-2.9
BTH_I2449		binding-protein-dependent transport system inner membrane component	-2.1
BTH_I2452		conserved hypothetical protein	-3.1
BTH_I2458		lipoprotein	-2.7
BTH_I2467		SpoVR family protein	-2.1
BTH_I2468		Protein of unknown function (DUF444) superfamily	-2.5
BTH_I2511	*pyrD*	dihydroorotate oxidase	-1.8
BTH_I2528		TetR family transcriptional regulator	-2.0
BTH_I2529		long-chain fatty acid-CoA ligase	-5.2
BTH_I2530		conserved hypothetical protein	-3.4
BTH_I2551		lipoprotein	-2.9
BTH_I2560		multidrug resistance protein	-1.9
BTH_I2669		hypothetical protein	-1.9
BTH_I2775		dihydropteroate synthase	-1.8
BTH_I2783	*carA*	carbamoyl phosphate synthase small subunit	-2.3
BTH_I2804		malonate transporter	-2.3
BTH_I2809		heat shock Hsp20	-2.1
BTH_I2826		hypothetical protein	-1.7
BTH_I2828		LacI family transcription regulator [	-2.8
BTH_I2830		ABC transporter permease	-2.2
BTH_I2841		conserved hypothetical protein	-2.7
BTH_I2860		Cysteine dioxygenase type I family	-1.8
BTH_I2880		Unknown protein	-2.7
BTH_I2900	*paaN*	phenylacetic acid degradation protein paaN	-2.1
BTH_I2901		beta-ketoadipyl CoA thiolase	-1.9
BTH_I3097	*paaG*	phenylacetate-CoA oxygenase subunit PaaA	-2.0
BTH_I3098		phenylacetate-CoA oxygenase subunit PaaB	-2.2
BTH_I3100		phenylacetic acid degradation protein PaaD	-1.9
BTH_I3111		orotate phosphoribosyltransferase	-2.2
BTH_I3148		hypothetical protein	-1.9
BTH_I3150		rare lipoprotein A family protein	-2.3
BTH_I3195		ribosomal protein S21-related protein	-2.4
BTH_I3217		hypothetical protein	-2.7

RNA-seq-based transcriptomics analysis was performed using total RNAs isolated from *B. thailandensis* E264 Δ*oxyR* mutant compared to the *B. thailandensis* E264 wild-type. The genes that are at least 1.6-fold changed in biological replicates were considered as significant. T6SS-4 genes and the *mnoT* (*bth_I1598*) gene were highlighted in yellow. qRT-PCR verified genes were

shown in boldface. [a] Fold change was defined by $2^{(\text{the gene expression ratio of } \Delta oxyR \text{ mutant to the } B.\ thailandensis\ E264 \text{ wild-type})}$.

Dataset S2. Bacterial strains, plasmids, and primers used in this study.

Strains or plasmids	Relevant characteristics	References
E. coli		
BL21(DE3)	Host for expression vector pET28a	Novagen
XL1 Blue	Host for expression vector pGEX6p-1	Novagen
TransB(DE3)	Host for expression vector pET15b	Novagen
JM109	*recA1 supE44 endA1 hsdR17 gyrA96 relA1 thi* Δ(*lac-proAB*)F′(*traD36 proABlacI*^{q} *lacΔZM15*)	Stratagene
S17-1 *λ pir*	*λ*-pir lysogen of S17-1, *thi pro hsdR hsdM*$^{+}$ *recA* RP4 2-Tc::Mu-Km::Tn7	Laboratory stock
SM10 *λ pir*	*λ*-pir lysogen of SM10, *thi pro hsdR hsdM*$^{+}$ *recA* RP4 2-Tc::Mu-Km::Tn7	Laboratory stock
B. thailandensis		
E264	Type strain (ATCC 700388); environmental isolate from Thailand, Str^{r}	62
Δ*hcp4*	*hcp4* gene deleted in *B. thailandensis* E264	This study
Δ*icmF4*	*icmF4* gene deleted in *B. thailandensis* E264	This study
Δ*clpV4*	*clpV4* gene deleted in *B. thailandensis* E264	This study
Δ*4clpV*	*clpV4*, *clpV1*, *clpV2* and *clpV6* genes deleted in *B. thailandensis* E264	This study
Δ*vgrG4a4b*	*vgrG4a* and *vgrG4b* genes deleted in *B. thailandensis* E264	This study
Δ*oxyR*	*oxyR* gene deleted in *B. thailandensis* E264	This study
Δ*tseM*	*tseM* gene deleted in *B. thailandensis* E264	This study
Δ*ahpC*	*ahpC* gene deleted in *B. thailandensis* E264	This study
Δ*katG*	*katG* gene deleted in *B. thailandensis* E264	This study
Δ*mnoT*	*mnoT* gene deleted in *B. thailandensis* E264	This study
Δ*mnoT*Δ*clpV4*	*mnoT* and *clpV4* genes deleted in *B. thailandensis* E264	
Δ*mnoT*Δ*tseM*	*mnoT* and *tseM* genes deleted in *B. thailandensis* E264	
Plasmid		
pME6032	Shuttle vector, Tc^{r}	62
pME6032-*hcp4*	*hcp4* under the control of chloramphenicol resistance gene promoter in plasmid pME6032	This study
pME6032-*oxyR*	*oxyR* under the control of chloramphenicol resistance gene promoter in plasmid pME6032	This study
pME6032-*tseM*	*tseM* under the control of chloramphenicol resistance gene promoter in plasmid pME6032	This study
pME6032-*tseM**	*tseM*$^{Q35R/H63A/N132R}$ under the control of chloramphenicol resistance gene promoter in plasmid pME6032	This study
pME6032-*mnoT*	*mnoT* under the control of chloramphenicol resistance gene promoter in plasmid pME6032	This study
pME6032-*clpV4*	*clpV4* under the control of chloramphenicol resistance gene promoter in plasmid pME6032	This study
pME6032-*clpV1*	*clpV1* under the control of chloramphenicol resistance gene promoter in plasmid pME6032	This study
pME6032-*clpV2*	*clpV2* under the control of chloramphenicol resistance gene promoter in plasmid pME6032	This study
pME6032-*clpV6*	*clpV6* under the control of chloramphenicol resistance gene promoter in plasmid pME6032	This study
pME6032-*vgrG4a*	*vgrG4a* under the control of chloramphenicol resistance gene promoter in plasmid pME6032	This study
pME6032-*vgrG4b*	*vgrG4b* under the control of chloramphenicol resistance gene promoter in plasmid pME6032	This study
pME6032-*icmF4*	*icmF4* under the control of chloramphenicol resistance gene	This study

	promoter in plasmid pME6032	
pME6032-*ahpC*	*ahpC* under the control of chloramphenicol resistance gene promoter in plasmid pME6032	This study
pME6032-*katG*	*katG* under the control of chloramphenicol resistance gene promoter in plasmid pME6032	This study
pET28a	Expression vector with N-terminal hexahistidine affinity tag, Km^r	Novagen
pET28a-*oxyR*	pET28a carrying *oxyR* coding region, Km^r	This study
pET28a-*fur*	pET28a carrying *fur* coding region, Km^r	32
pGEX6p-1	Expression vector with N-terminal GST tag, Amp^r	Novagen
pGEX6p-1-*tseM*	pGEX6p-1 carrying *tseM* coding region, Amp^r	This study
pGEX6p-1-*tseM**	pGEX6p-1 carrying $tseM^{Q35R/H63A/N132R}$ coding region, Amp^r	This study
pET15b	Expression vector with N-terminal hexahistidine affinity tag, Amp^r	Novagen
pET15b-*tseM*	pET15b carrying *tseM* coding region, Amp^r	This study
pET15b-*mnoT*	pET28a carrying *mnoT* coding region, Amp^r	This study
pDM4-*pheS*	Suicide vector, *mob*RK2, *ori*R6K, *pir*, *pheS*, Cm^r	62
pDM4-*pheS*-Δ*icmF4*	Construct used for in-frame deletion of *icmF4*, Cm^r	This study
pDM4-*pheS*-Δ*oxyR*	Construct used for in-frame deletion of *oxyR*, Cm^r	This study
pDM4-*pheS*-Δ*mnoT*	Construct used for in-frame deletion of *mnoT*, Cm^r	This study
pDM4-*pheS*-Δ*tseM*	Construct used for in-frame deletion of *tseM*, Cm^r	This study
pDM4-*pheS*-Δ*clpV1*	Construct used for in-frame deletion of *clpV1*, Cm^r	This study
pDM4-*pheS*-Δ*clpV2*	Construct used for in-frame deletion of *clpV2*, Cm^r	This study
pDM4-*pheS*-Δ*clpV4*	Construct used for in-frame deletion of *clpV4*, Cm^r	This study
pDM4-*pheS*-Δ*clpV6*	Construct used for in-frame deletion of *clpV6*, Cm^r	This study
pDM4-*pheS*-Δ*hcp4*	Construct used for in-frame deletion of *hcp4*, Cm^r	This study
pDM4-*pheS*-Δ*vgrG4a4b*	Construct used for in-frame deletion of *vgrG4a4b*, Cm^r	This study
pDM4-*pheS*-Δ*ahpC*	Construct used for in-frame deletion of *ahpC*, Cm^r	This study
pDM4-*pheS*-Δ*katG*	Construct used for in-frame deletion of *katG*, Cm^r	This study

Primers	**5'-3' sequence**	**Function**
D*oxyR*-F1	GGACTAGTGGGTATGCCCGCTCATCGAGGAAAG (Spe I)	To generate pDM4-*pheS*-Δ*oxyR*
D*oxyR*-R1	GACGATGTACTTCAGTTCAGTAAGC	
D*oxyR*-F2	GCTTACTGAACTGAAGTACATCGTCGACATCCCGGCTACGGT GAATTG	
D*oxyR*-R2	CGGGATCCCTATGCCACGCCATGCGGATGAACA (BamH I)	
oxyR-F	CCGGAATTCATGACGCTTACTGAACTGAAGTAC (EcoR I)	To generate pME6032-*oxyR* and pET28a-*oxyR*
oxyR-R1	CGGGGTACCTCAATTCACCGTAGCCGGGATGTC (Kpn I)	To generate pME6032-*oxyR*
oxyR-R2	ACGCGTCGACTCAATTCACCGTAGCCGGGATGTC (Sal I)	To generate pET28a-*oxyR*
D*clpV4*-F1	CTAGACTAGTCATCGAGGACGACGATCACC (Spe I)	To generate pDM4-*pheS*-Δ*clpV4*
D*clpV4*-R1	GCGGCCGAGACAGTTGAATATG	
D*clpV4*-F2	CATATTCAACTGTCTCGGCCGCATCATCCCGACGAAACGACC	
D *clpV4*-R2	GGAAGATCTAGTCGTAGTACTCGAGCGGAATC (BglI I)	
clpV4-F	GGAGGTACCGTGAATCGCGAACGCATATTCAAC (Kpn I)	To generate pME6032-*clpV4*
clpV4-R	CGGAGATCTTCAGACGCATGACGGTTCTCCC (Bgl II)	
DtseM-F1	GGACTAGTCGACTGGACCAATCAGAACACGCA (Spe I)	To generate pDM4-*pheS*-Δ*tseM*
DtseM-R1	TCGCGTCATTCGTCTCCTCGGCCCATTGCTCACAAAAGATTG AAACGG	
DtseM-F2	GCCGAGGAGACGAATGACGCGA	

DtseM-R2	GAAGATCTTCGCCCTCTTATCGCTATCCGTC (Bgl II)	
tseM-F1	CGCGGATCCTTGCGTCGGCGTCAGCGCGCTTC (BamH I)	To generate pGEX6p-1-*tseM*
tseM-R1	CCGCTCGAGTTACTTGCGCGCCTCGCTCAGC (Xho I)	
tseM-F2	GGGAATTCCATATGTTGCGTCGGCGTCAGCGCGCTTC (Nde I)	To generate pET15b-*tseM*
tseM-R2	CGCGGATCCTTACTTGCGCGCCTCGCTCAGC (BamH I)	
tseM-F3	CGGGGTACC TTGCGTCGGCGTCAGCGCGCTTC (Kpn I)	To generate pME6032-*tseM*
tseM-R3	GAAGATCTTTACTTGCGCGCCTCGCTCAGC (Bgl II)	
tseMQ35R-F	GGCGCGCCCGTTTC**G**ATCTTTTGTGAGCA	To generate mutant $tseM^{Q35R}$ fragment
tseMQ35R-R	TGCTCACAAAAGAT**C**GAAACGGGCGCGCC	
tseMH63A-F	TCGATGAGCAGC**GC**TGCGCAACTGGGG	To generate mutant $tseM^{H63A}$ fragment
tseMH63A-R	CCCCAGTTGCGCA**GC**GCTGCTCATCGA	
tseMN132R-F	GGCCGAGGAGACGA**GG**GACGCGACGCTGAG	To generate mutant $tseM^{N132R}$ fragment
tseMN132R-R	CTCAGCGTCGCGTC**CC**TCGTCTCCTCGGCC	
D*icmF4* -F1	CTAGACTAGTATCAGCCTCTGGCTCGATTCGCAG (Spe I)	To generate pDM4-*pheS*-Δ*icmF4*
D*icmF4*-R1	CGAATACTCTCAAGCTCGTGCG	
D*icmF4*-F2	CGCACGAGCTTGAGAGTATTCGTGATGCGTCGAGCATCGGTATTC	
D*icmF4*-R2	GGAAGATCTCTGATTCAAGCGGCTTTCGCGAC (Bgl II)	
icmF4-F	CCGGAATTCATGATCCGCACGAGCTTGAGAG (EcoR I)	To generate pME6032-*icmF4*
icmF4-R	GGAAGATCTTCACGACGGACACCTGAACGACTG (Bgl II)	
D*hcp4* -F1	CTAGACTAGTTTCAAGACCTACGGCTGGTG (Spe I)	To generate pDM4-*pheS*-Δ*hcp4*
D*hcp4*-R1	CCGGGATATTGCGAATCGGTC	
D*hcp4*-F2	GACCGATTCGCAATATCCCGGCCGATCTAACCCGTCGGAAG	
D*hcp4*-R2	GGAAGATCTGAGAACATCACCGGCAGCTTG (Bgl II)	
hcp4-F1	CTATCGAGCTCATGGCAAATGCTTTGGTTGATTAC (Sac I)	To generate pME6032-*hcp4*
hcp4-R1	GGAAGATCTGATCGGGGCGTTCTGCTTGAGG (Bgl II)	
D*clpV1*-F1	CTAGACTAGTGCATTACACCGAGCAGATCATCGC (Spe I)	To generate pDM4-*pheS*-Δ*clpV1*
D*clpV1*-R1	CTTCAGGGGCGTGCTCATCGGTTA	
D*clpV1*-F2	TAACCGATGAGCACGCCCCTGAAGTCGATCACATCCTGAACGGCACG	
D*clpV1*-R2	GGAAGATCTACGCAACGGGTGTCATCCGCTTC (Bgl II)	
D*clpV2*-F1	CTAGACTAGTGCGGCAATCGACTTGAGCGCAATG (Spe I)	To generate pDM4-*pheS*-Δ*clpV2*
D*clpV2*-R1	AACCGGAAAATGGCGCGTCGTGTCC	
D*clpV2*-F2	GGACACGACGCGCCATTTTCCGGTTCGCTTCTTGACGATGCCGTGGTT	
D*clpV2*-R2	GGAAGATCTCGAGATCGTCCTGAAGCCGCTTTC (Bgl II)	
D*clpV6*-F1	CTAGACTAGTGCATCTGACCGAGTATGCGTACGA (Spe I)	To generate pDM4-*pheS*-Δ*clpV6*
D*clpV6*-R1	CGTCGCCTGCTCCAATGTCTCGT	
D*clpV6*-F2	ACGAGACATTGGAGCAGGCGACGCCGAAGACGGCCAGTTCGTTTATC	
D*clpV6*-R2	GGAAGATCTCGCGTTCTCCTGAAACCGATACTGG (Bgl II)	
D*mnoT*-F1	GGACTAGTTCTCGGGAGGCGGAATG (Spe I)	To generate pDM4-*pheS*-Δ*mnoT*
D*mnoT*-R1	GCGGCAAGTTCATGGGAC	
D*mnoT*-F2	GTCCCATGAACTTGCCGCCTACGTGTTTCACCCTTATCCA	
D*mnoT*-R2	GGAAGATCTGGAAGATCTGAACCACGCGAGATGCC (Bgl II)	

mnoT-F1	CCGGAATTCATGTCCCATGAACTTGCCGCG (EcoR I)	To generate pME6032-*mnoT*
mnoT-F2	GGAATTCCATATGATGTCCCATGAACTTGCCGCG (Nde I)	To generate pET15b-*mnoT*
mnoT-R	CGCGGATCCTCACAGCGACCATTTCAACTC (BamH I)	To generate pME6032-*mnoT* and pET15b-*mnoT*
D*ahpC*-F1	CTAGACTAGTGAGCCTCGTGAACCAGCC (Spe I)	To generate pDM4-*pheS*-Δ*ahpC*
D*ahpC*-R1	GTCCGTTTGCTTTTCTTCGTGGTTGTTGAA	
D*ahpC*-F2	ACGAAGAAAAGCAAACGGACGAACTCTGCC	
D*ahpC*-R2	GGAAGATCTGTGAACGTGAAGGCGAAGAC (Bgl II)	
ahpC-F	CGGGGTACCATGAAGACCGTGGGCGATAAA (Kpn I)	To generate pME6032-*ahpC*
ahpC-R	GGAAGATCTTTACAGCGTCGCGCCGCCGAT (Bgl II)	
D*vgrG4a4b*-F1	CTAGTCTAGAATACGTCGGTTACGGCAAGG (Xba I)	To generate pDM4-*pheS*-Δ*vgrG4a4b*
D*vgrG4a4b*-R1	TCAGACGCATGACGGTTCTC	
D*vgrG4a4b*-F2	GAGAACCGTCATGCGTCTGAGGACGTGGGCATTGATCTGAAG	
D*vgrG4a4b*-R2	GGAAGATCTCCTTGAATGCGATCACGAGC (Bgl II)	
vgrG4a-F	CGGGGTACCATGCGTCTGATCGAACTGCG (Kpn I)	To generate pME6032-*vgrG4a*
vgrG4a-R	GGAAGATCTTCAGCTCTTCACTTGCATGC (Bgl II)	
vgrG4b-F	CGGGGTACCATGCGTCTGATCGAACTACG (Kpn I)	To generate pME6032-*vgrG4b*
vgrG4b-R	GGAAGATCTTCAGTTCTTCGTCTGCATCCCG (Bgl II)	
clpV1-F	CGGGGTACCATGAGCACGCCCCTGAAGAC (Kpn I)	To generate pME6032-*clpV1*
clpV1-R	GGAAGATCTCGCGCGCCGGCCTTACTCGA (Bgl II)	
clpV2-F	CGGGGTACCCGATTAATGTCGTGCCTTTC (Kpn I)	To generate pME6032-*clpV2*
clpV2-R	GGAAGATCTTCAAGAAGCGCGCAGGACAA (Bgl II)	
clpV6-F	CGGGGTACCGGAATCGCCATGTCCGATAT (Kpn I)	To generate pME6032-*clpV6*
clpV6-R	CGCGGATCCTCACGTCGCACCCTCCTCTT (BamH I)	
D*katG*-F1	GGACTAGTCCGACCTGAAGCAGGAGACGATG (Spe I)	To generate pDM4-*pheS*-Δ*katG*
D*katG*-R1	GAACGGGCACTTCGCTTCATTCG	
D*katG*-F2	CGAATGAAGCGAAGTGCCCGTTCCAGGCGCTGACCAACGACTTCT	
D*katG*-R2	CGGGATCCCAGCGTGTACGTATCGGCAAGCAGG (BamH I)	
katG-F	CGGGGTACCATATCAATGGAATTCATCGA (Kpn I)	To generate pME6032-*katG*
katG-R	GGAAGATCTTTCCGCTTACTTGCCTTCTG (Bgl II)	
P_{T6}-oxyR-F-5'biotin	GTTTGTAAGAAAAAATTATTTCCG	EMSA
P_{T6}-oxyR-R-3'biotin	CGGCGTCCGGGAAAATATTCCACG	EMSA
P_{T6}-oxyR-F	GTTTGTAAGAAAAAATTATTTCCG	EMSA
P_{T6}-oxyR-R	CGGCGTCCGGGAAAATATTCCACG	EMSA
Q16SRNA-F	AACCTTACCTACCCTTGA	RT-PCR
Q16SRNA-R	GCTCGTTGCGGGACTTA	RT-PCR
Q*clpV4*-F	TGTCGCATTCGGGGCTCA	RT-PCR
Q*clpV4*-R	TCGCCGCCGAACAGCA	RT-PCR
Q*hcp4*-F	GGGTGAGCACATCCAGAA	RT-PCR
Q*hcp4*-R	GAACGACGAGACGAGGC	RT-PCR
Q*icmF4*-F	TGTCGCATTCGGGGCTCA	RT-PCR
Q*icmF4*-R	TCGCCGCCGAACAGCA	RT-PCR

Q*vgrG4*-F	GCAAGGGCTGGGGTGT	RT-PCR
Q*vgrG4*-R	CGTAAGGCGTCGGGTTTT	RT-PCR
Q*tseM*-F	CGCCCGTTTCAATCTTT	RT-PCR
Q*tseM*-R	GCGTCACCTGCTCCTTCA	RT-PCR
Q*mnoT*-F	CGATTTGCGAGCGGAGTC	RT-PCR
Q*mnoT*-R	TCCGCCGTGTTGTAGGTC	RT-PCR
Q*katG*-F	GCCGATCAAGCAGAAATACG	RT-PCR
Q*katG*-R	CGAGCCCCAGTAGACATCC	RT-PCR
Q*ahpC*-F	CCTTCGCGGCGAAGAGC	RT-PCR
Q*ahpC*-R	CGCAGAAGTGGCACTTAC	RT-PCR
QBTH_II2141 F	TCGCTACAAGCCGCTGACCC	RT-PCR
QBTH_II2141 R	CCCGAAGCCGAGCAGAAACA	RT-PCR
QBTH_I1442-F	AAGGTTCATCAGACGTTCATGCC	RT-PCR
QBTH_I1442-R	TCGGTGTACGGATAGTCGTTGCG	RT-PCR
QBTH_II1726F	CTGGCCGCCTGGCTCTTGAT	RT-PCR
QBTH_II1726R	CCGACCATTGCGATGTTGAT	RT-PCR
QBTH_II0421F	CGGGGCGAGCGCCGCGCG	RT-PCR
QBTH_II0421R	GGCGCGGAAAAGAACACG	RT-PCR
QBTH_II0919F	CGCGTCCGGCGACGC	RT-PCR
QBTH_II0919R	GATCGGTCGTCGATTCG	RT-PCR
QBTH_II1073F	CGCGCCGTCGACATC	RT-PCR
QBTH_II1073R	CCGAGCCGTCGCCCTGC	RT-PCR
QBTH_I0165F	CGACGATCGTCTCCGTGC	RT-PCR
QBTH_I0165R	GCACGTCGCCGTTGCCGG	RT-PCR
QBTH_I1845F	CGAGCCGCTGCACGTG	RT-PCR
QBTH_I1845R	CCTGCGTGTACTCGCG	RT-PCR
QBTH_II0279F	CGCGGCCGCAACTACTC	RT-PCR
QBTH_II0279R	TCGAACGCGCCGAGCGA	RT-PCR

* Str^r, Cm^r, Km^r, Tc^r and Amp^r represent resistance to streptomycin, chloramphenicol, kanamycin, tetracycline and ampicillin, respectively. Underlined sites indicate restriction enzyme cutting sites added for cloning. Letters in boldface denote the mutation sites in overlap PCR for site-directed mutagenesis.